Multiscale Physics Challenges for Plasma-Facing Materials

N.M. Ghoniem (UCLA) and B. Wirth (UCB)

APS-DPP Meeting

Mini-conference: "The first few microns of the first wall"

November 16-20, 2007

Orlando, Florida

Lecture Outline

- Research Approach and the Materials Environment;
- Plasma Physics – Materials Science Analogies;
- The new kid on the block: Multiscale Modeling;
- A few Basics: collision cascades. Defects & Microstructure;
- Surface and Bulk Phenomena;
- Fundamental Equations and Algorithms;
- Modeling Challenges and Limitations.

Material-Plasma Interfacing

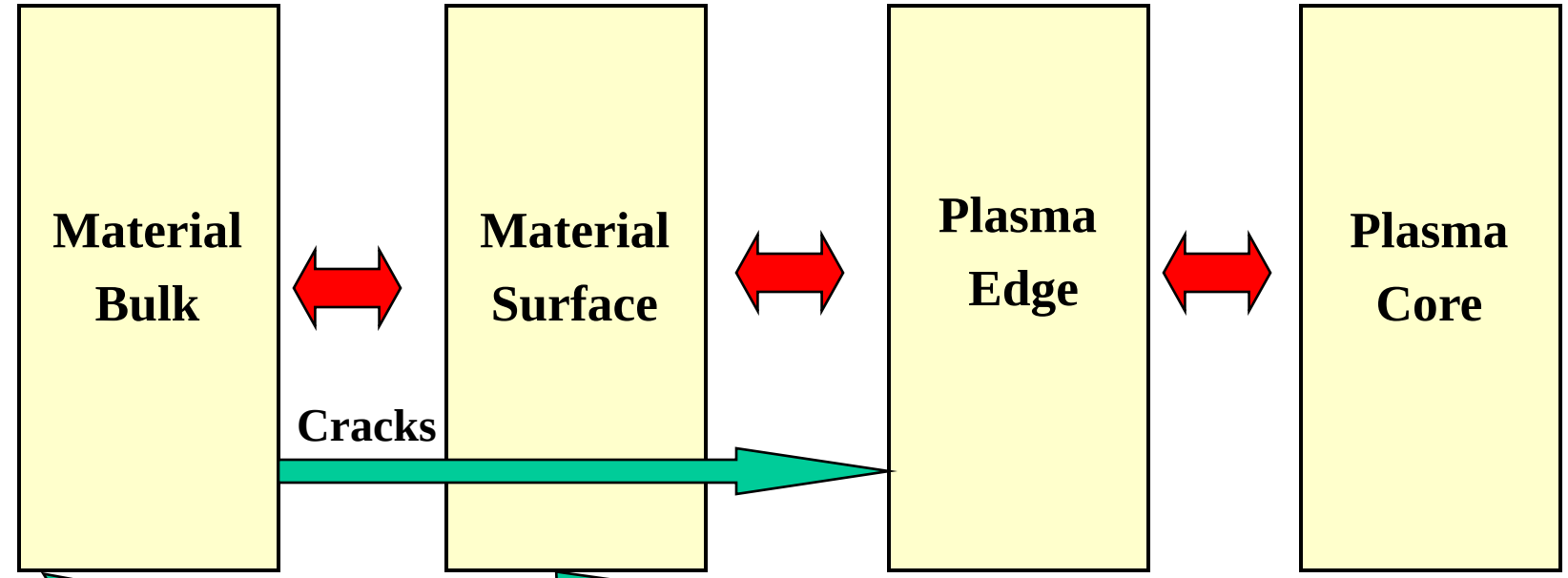

- Ab initio;
- MD
- KMC
- DD
- Rate Theory
- FEM

- VFTRIM;
- REDEP
- HEIGHTS
- BPHI-3D
- UEDGE-2D

- Transport;
- Turbulence;
- MHD;
- Confinement;
- Islands, Stability & Oscillations.

Correspondence & Analogy

Phenomenon	Plasma	Material
Density & Degrees of Freedom per cm^3	❑10^{14} - 10^{16}	❑10^{23}
Forces	❑***Long-range***: Coulomb, Electromagnetic	❑***Short-range***: Atomic > Pair, Many-body ❑***Long-range***: Elastic
Particle Methods	❑Particle-Particle (P-P); ❑Particle-Field (PIC); ❑KMC	❑Particle-Particle (MD); ❑Particle-Field (DD-FEM); ❑KMC, Lattice MC, Event MC.
Transport & Continuum	❑Collisions & Fokker-Planck; ❑Fluid, MHD ❑Reaction Cross-sections; ❑Turbulence	❑ Microstructure Evolution & Fokker-Planck*; ❑Elasticity; ❑Rate Theory; ❑Plasticity
Instabilities	❑***Space***: Islands, Coherent Structures; ❑***Time:*** Oscillations, Disruptions	❑***Space***: Self-organization, segregation; ❑***Time:*** shear bands, cracks.

*H. Huang and N.M. Ghoniem, "Formulation of a Moment Method for n-dimensional Fokker-Planck Equations", *Phys. Rev. E*, **51, 6**: 5251-5260, 1995.

Correspondence & Analogy

Biot-Savart

$$d\vec{B} = \frac{\mu_o}{4\pi}\frac{Id\vec{s}\times\hat{r}}{r^2}$$

$$\vec{B} = \frac{\mu_o I}{4\pi}\oint\frac{d\vec{s}\times\hat{r}}{r^2}$$

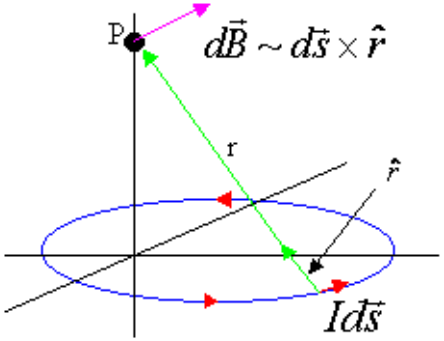

Electromagnetics		Dislocation Dynamics	
Magnetic intensity	H_i	Strain	ε_{ij}
Magnetic induction	B_i	Stress	σ_{ij}
Current density	J_i	Incompatibility tensor	η_{ij}
Permeability	μ	Elastic constants	$E,\ \nu$
Vector potential	A_i	Stress function	χ_{ij}
Current	I	Burgers vector	b_i
Maxwell's Equation:	$\in_{ijk} H_{k,j} = J_i$	Incompatibility Equation:	$-\in_{ikl}\in_{jmn}\varepsilon_{nl,km} = \eta_{ij}$

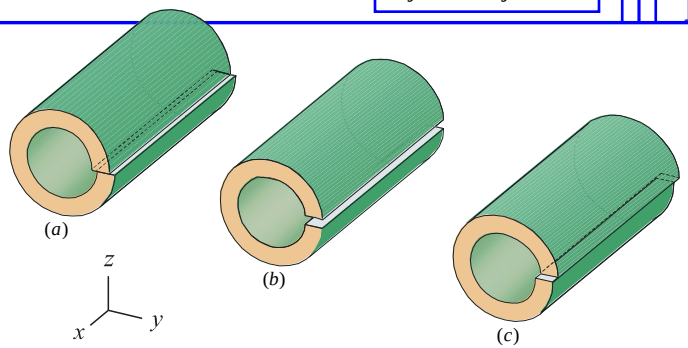

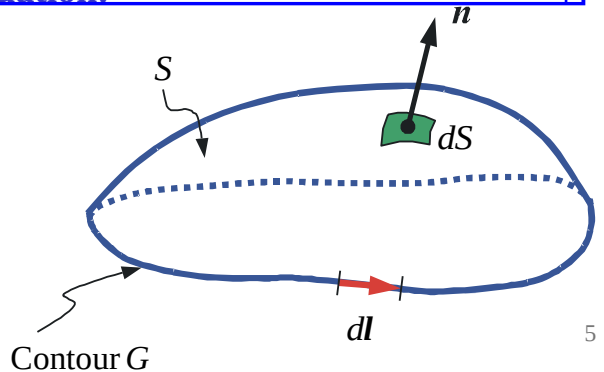

Approach and Materials Environment - MFE

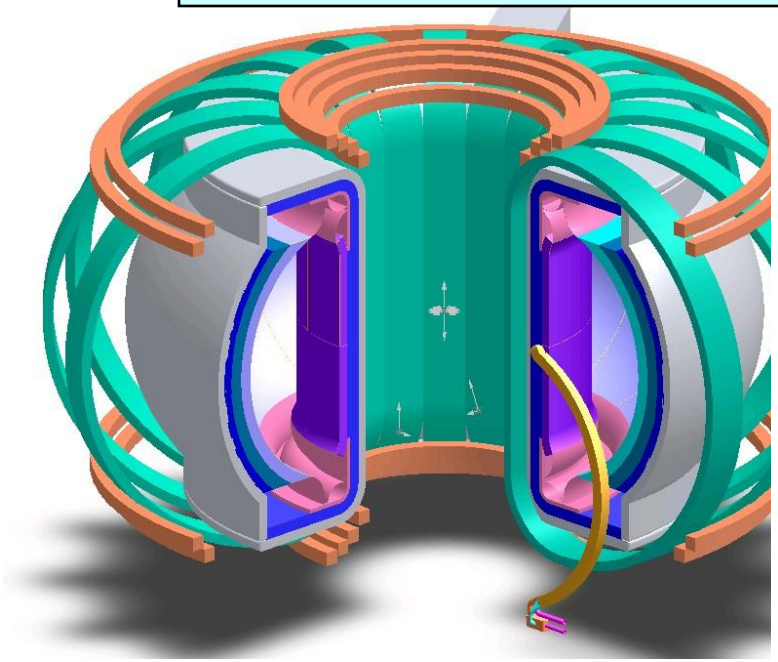

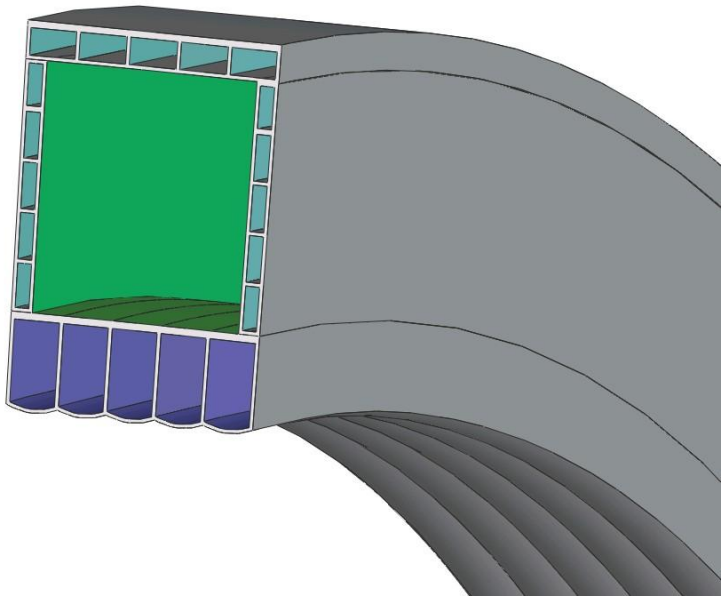

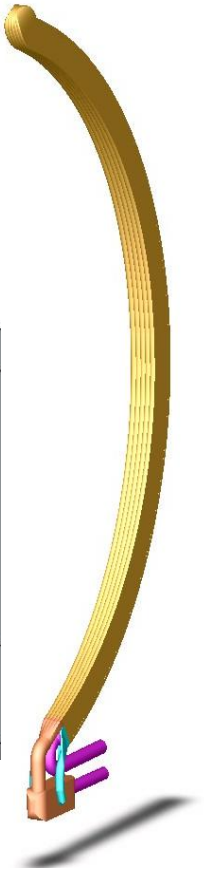

Environment

- *Heat Flux: FW ~1 MW/m^2; Divertor ~5 –15 MW/m^2*
- *Neutron Flux: ~ 3 – 5 MW/m^2*
- *Particle Flux: Divertor ~10^{21}-10^{22} m^{-2}s^{-1}*
- *Mechanical Loads: Pressure ~ 2-5 MPa*

Approach

- *Predictive;*
- *Physics-Based;*
- *Computational Design of Materials;*
- *Experimentally-verifiable at Scale Interfaces.*

ACCELERATED MATERIAL DEVELOPMENT METHODOLOGY

- **Traditional** Physical Methodology:

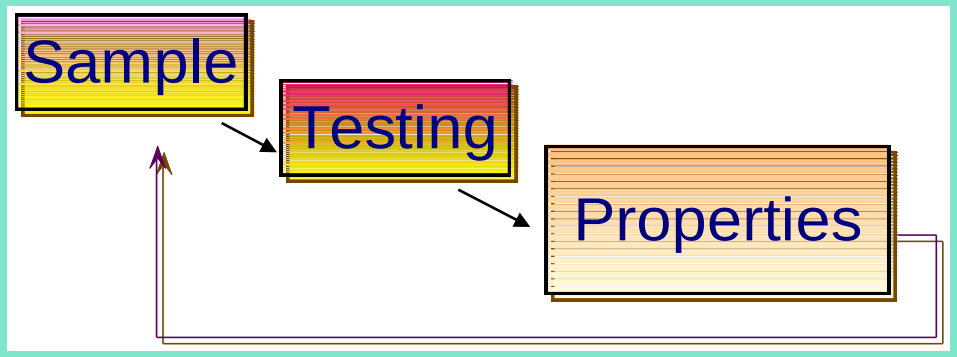

- **Digital** Analog Methodology:

INTEGRATED MODELING INPUT

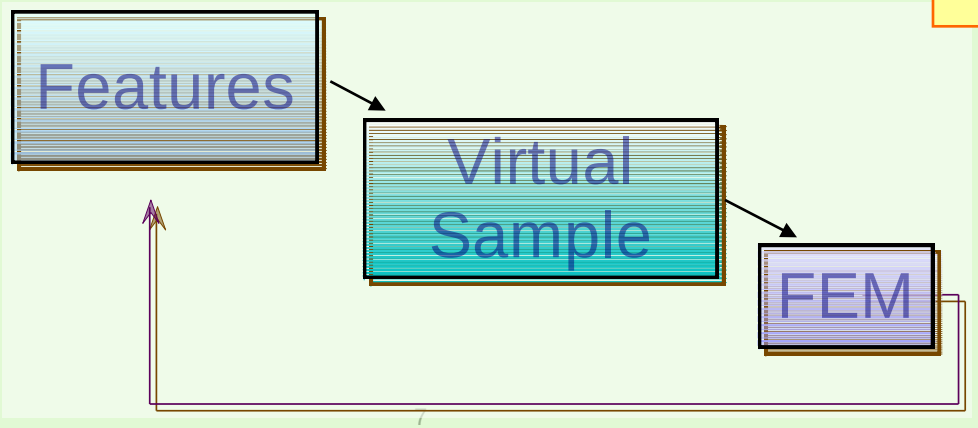

Multi-scale Modeling Strategy

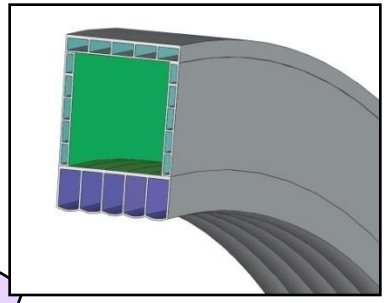

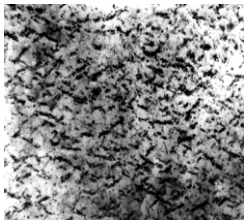

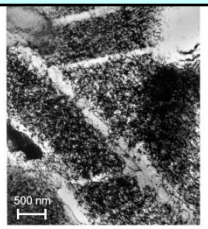

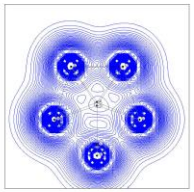

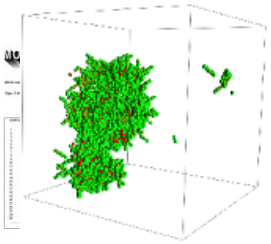

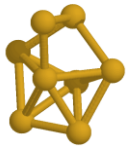

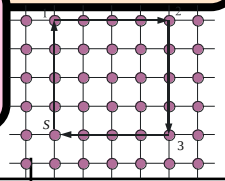

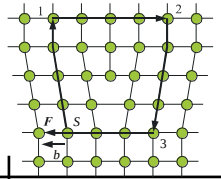

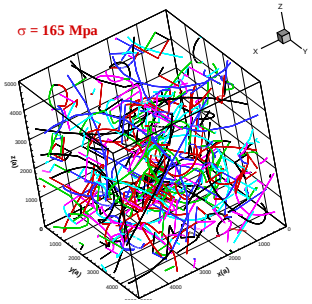

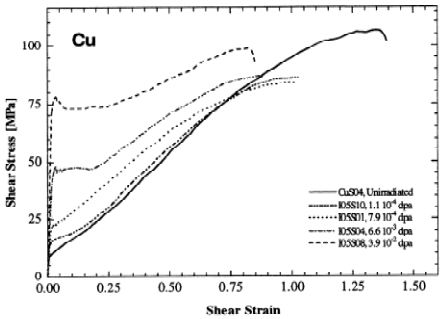

Space

m

m

μ m

n m

Quantum Mechanics

Classical MD

Monte Carlo

Dislocation Dynamics

Statistical Mechanics

Continuum Mechanics

f s

p s

n s

μ s

m s

s

k s

Time

FUSION STRUCTURAL COMPONENT DEVELOPMENT LOGIC

Multi-Scale Material Modeling

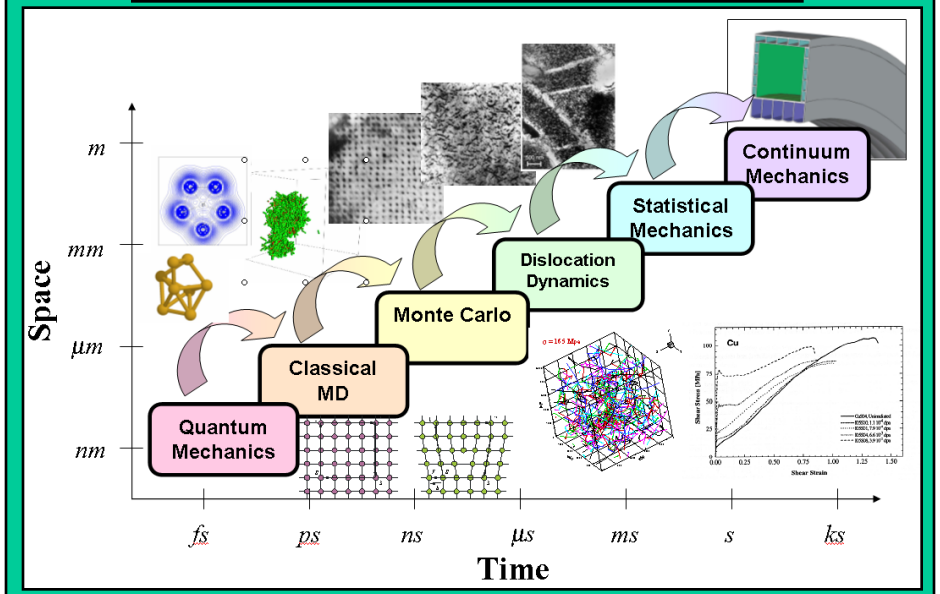

Experiments and Tests

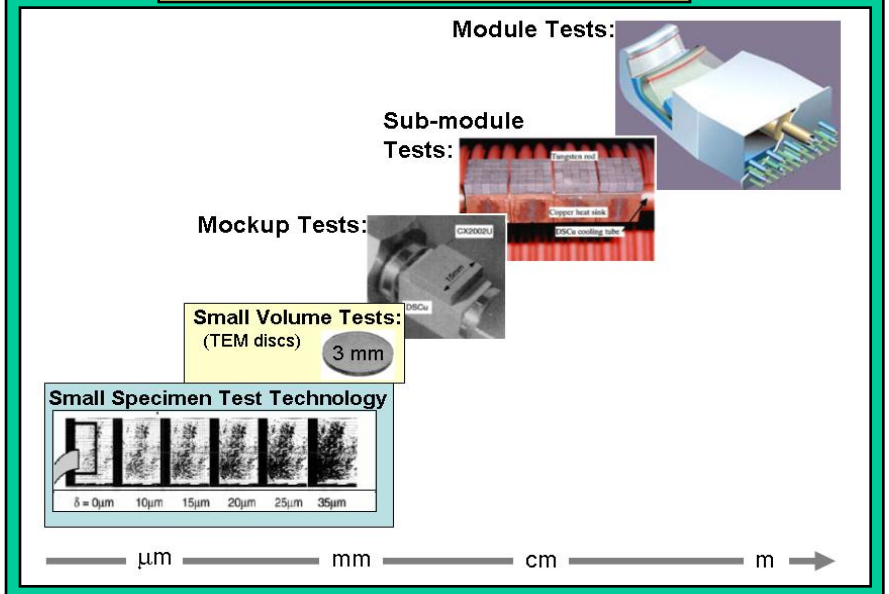

PROPERTIES:

Tensile, fatigue, toughness, creep, crack growth, swelling…

Structural Performance and Reliability Assessment

Defects & the Microstructure

MONOGRAPHS ON THE PHYSICS AND CHEMISTRY OF MATERIALS • 63

OXFORD SCIENCE PUBLICATIONS

In materials, critical phenomena such as phase transitions, plastic deformation, and fracture are intimately related to self-organization. Understanding the origin of spatio-temporal order in systems far from thermal equilibrium and the selection mechanisms of spatial structures and their symmetries is a major theme of present day research on the structure of continuous matter. Furthermore, the development of methods for producing spatially-ordered and self-assembled microstructure in solids by non-equilibrium methods opens the door to many technological applications. There is an increasing demand for a better understanding of new materials from a more fundamental point of view. In order to describe and understand the behavior of such materials, dynamical concepts related to non-equilibrium phenomena, irreversible thermodynamics, nonlinear dynamics, and bifurcation theory, are required. The generic presence of defects and their crucial influence on pattern formation and critical phenomena in extended systems is now well-established. Similar to observations in hydrodynamical, liquid crystal, and laser systems, defects in materials have a profound effect. We found it thus timely to develop a unified presentation of tools, concepts, and methods that are useful to material scientists and engineers. Although specialized treatments of various topics covered in this book are available, we feel that a comprehensive approach may give the reader a higher vantage point. Hence, emphasis is placed on combining the basic physical, mathematical, and computational aspects with technological applications within the material's life-cycle, from processing, degradation to eventual failure.

Nasr M. Ghoniem is a Professor in the Materials Science and Engineering Department, University of California at Los Angeles.

Daniel D. Walgraef is Director of Research at the Belgian National Fund for Scientific Research, Brussels.

'A very useful resource introducing students in the physical sciences to the theoretical background behind specific calculations, and students in the mathematical sciences to interesting applications.' Kaushik Bhattacharya, California Institute of Technology

'The topic of instabilities and self-organization is rich in theoretical interest and practical motivation, and it is timely.' Robert Rudd, Lawrence Livermore National Laboratory

Cover Image: The cover shows the self-organized structure and magnificent colors of a cactus plant. The picture was taken by N. Ghoniem in spring 2005. Inspiration provided by Matthew Koerner.

ALSO PUBLISHED BY OXFORD UNIVERSITY PRESS

V. Bulatov and W. Cai: Computer simulations of dislocations
M. Finnis: Interatomic forces in condensed matter
J. C. H. Spence: High-resolution electron microscopy (third edition)
L.-M. Peng, S. L. Dudarev, and M. J. Whelan: High-energy electron diffraction and microscopy

OXFORD
UNIVERSITY PRESS
www.oup.com

ISBN 978-0-19-929869-3

Ghoniem and Walgraef

Instabilities and Self-Organization in Materials
Volume I: Fundamentals of Nanoscience

OXFORD

Instabilities and Self-Organization in Materials

Volume I: Fundamentals of Nanoscience

Nasr Ghoniem and Daniel Walgraef

Defects & the Microstructure

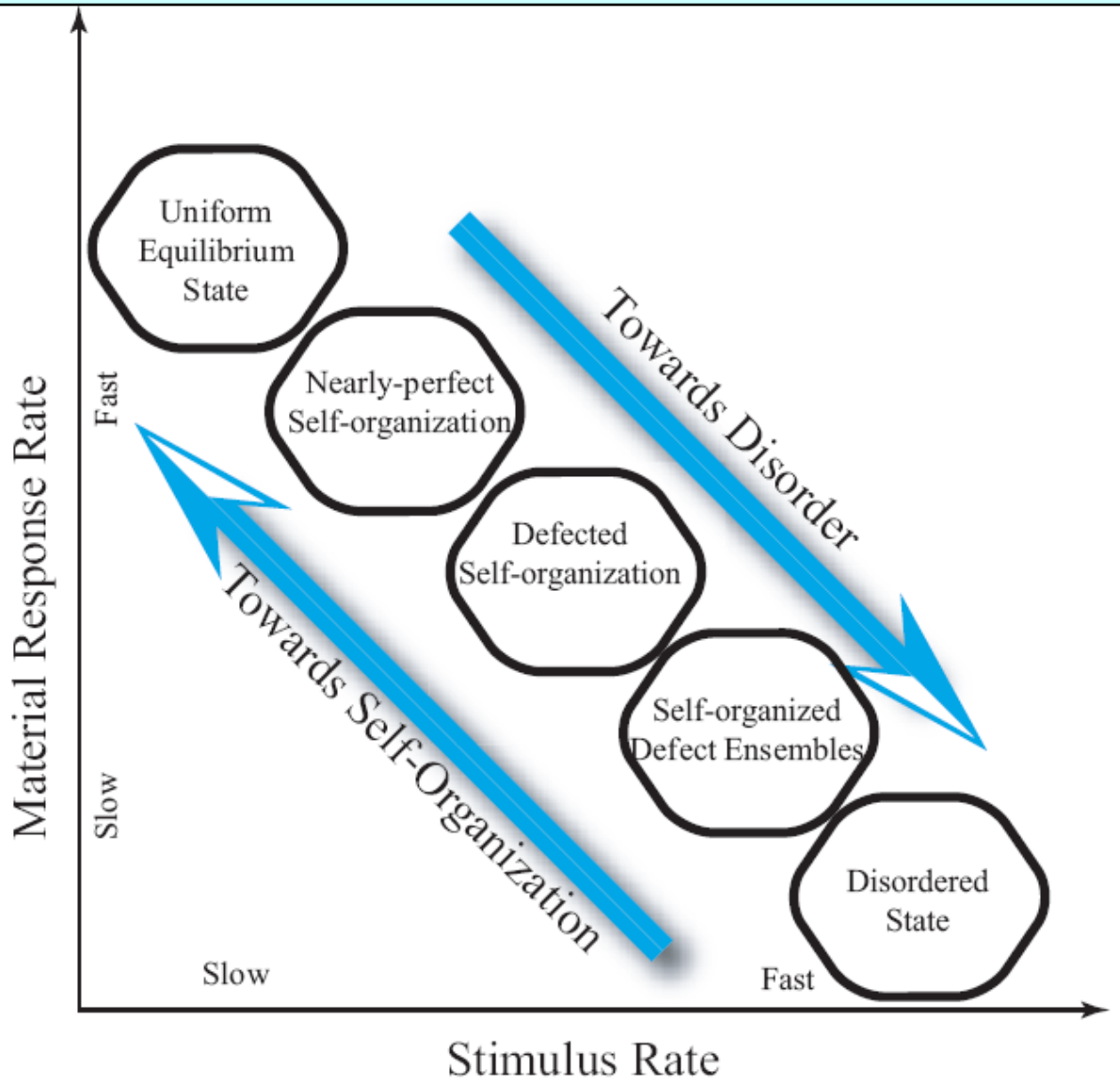

Point & Line Defects

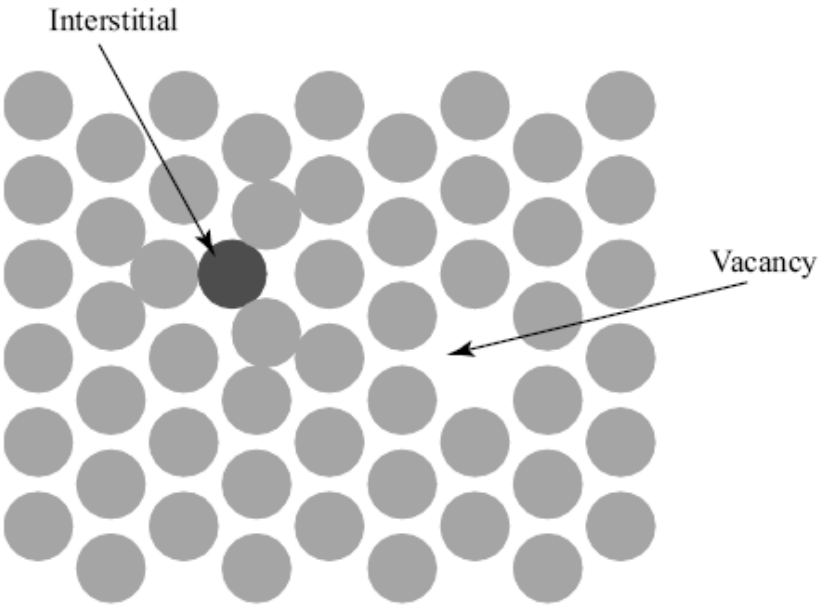

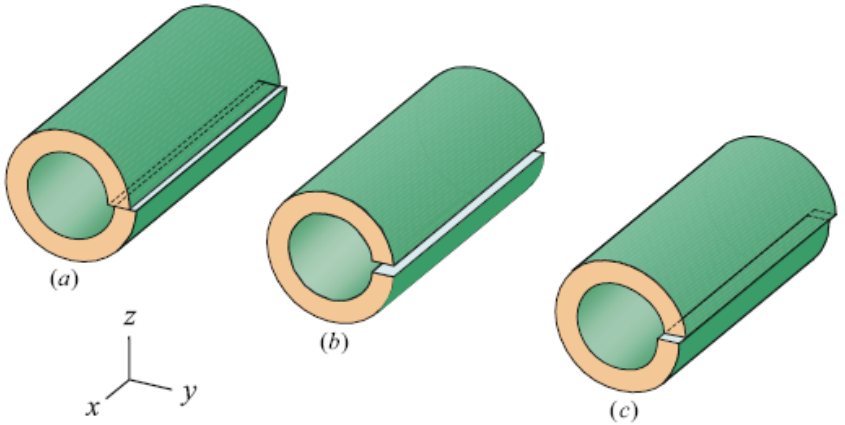

Figure 3.1: Dislocation types in materials

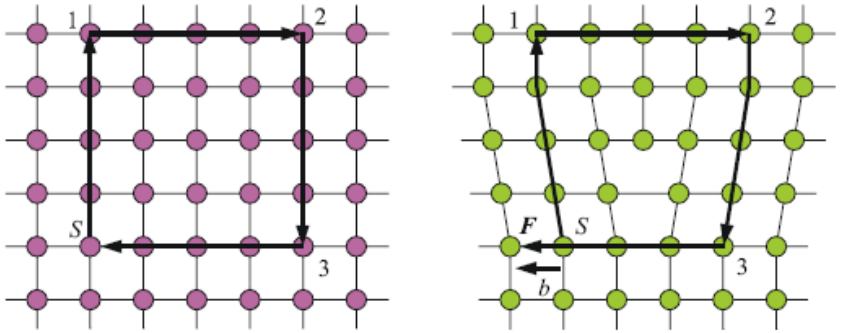

Figure 3.2: Burgers circuit for an edge dislocation

Interfacial Defects & Boundaries

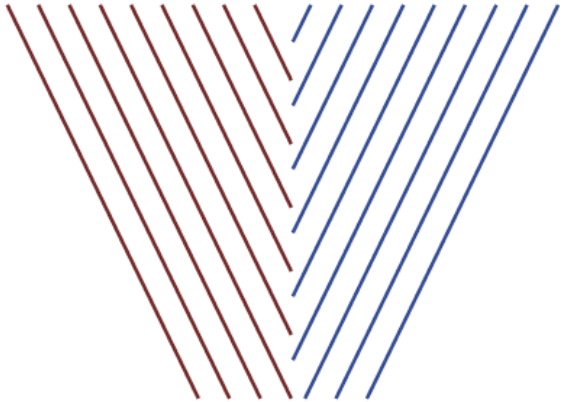

Figure 3.6: Stable tilt boundary

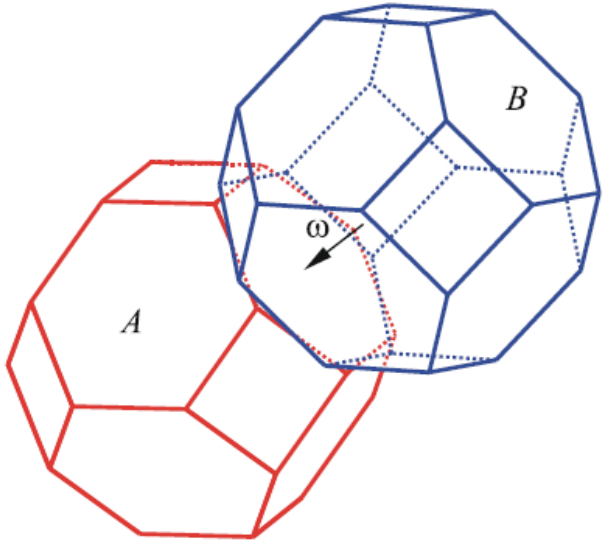

Figure 3.7: Twist boundary between grains

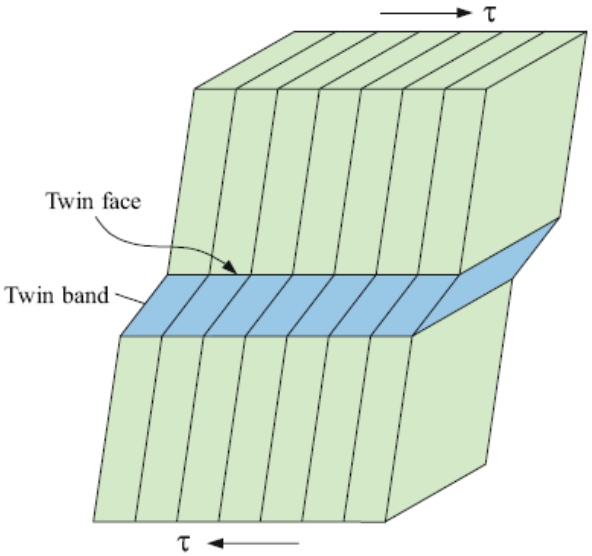

Figure 3.9: Twin band geometry

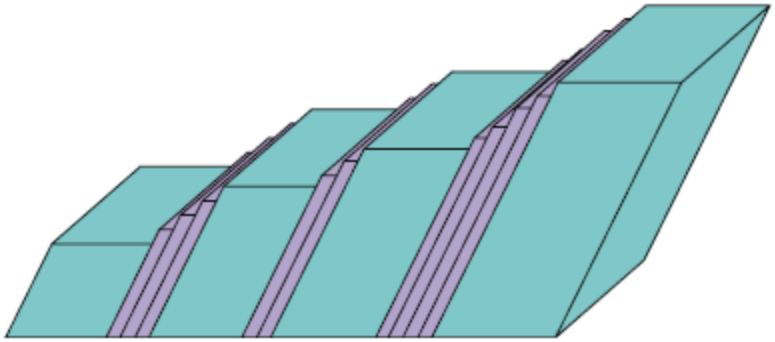

Figure 3.8: Slip band geometry

Defects & the Microstructure

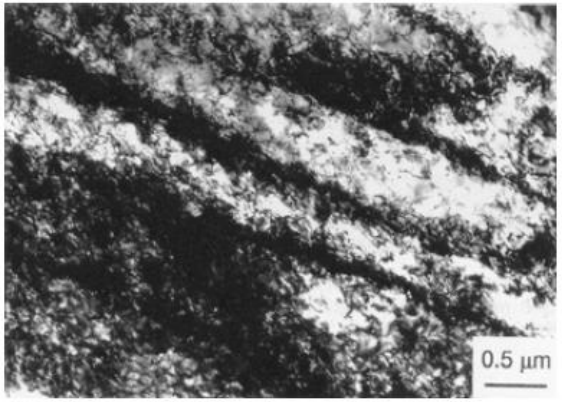

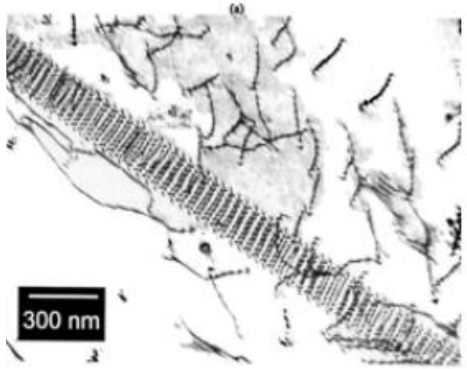

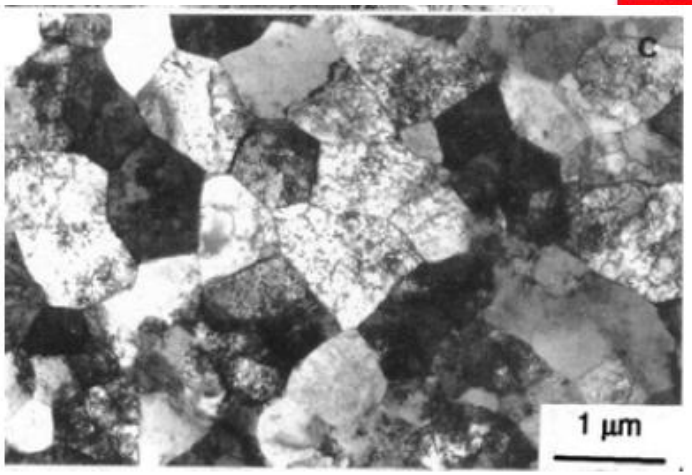

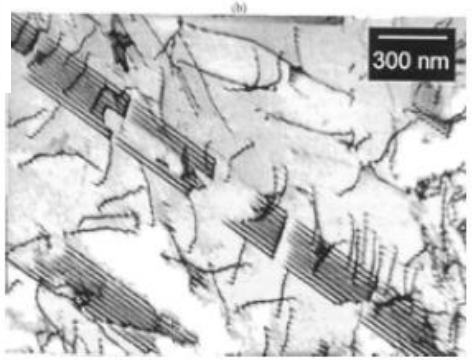

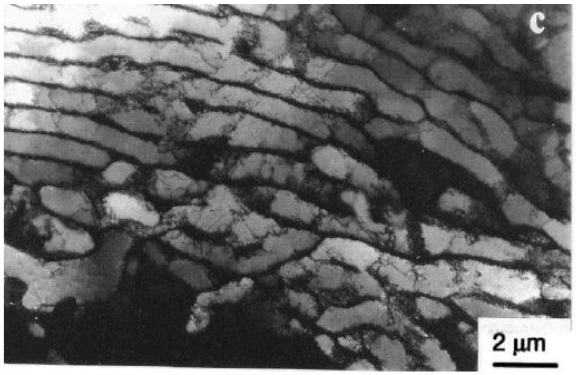
c
2 μm


b
1 μm

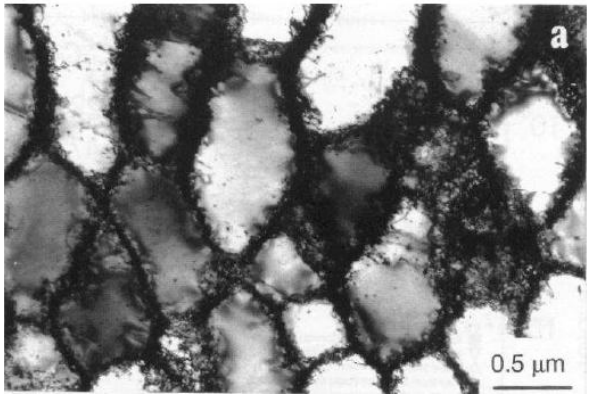
a
0.5 μm

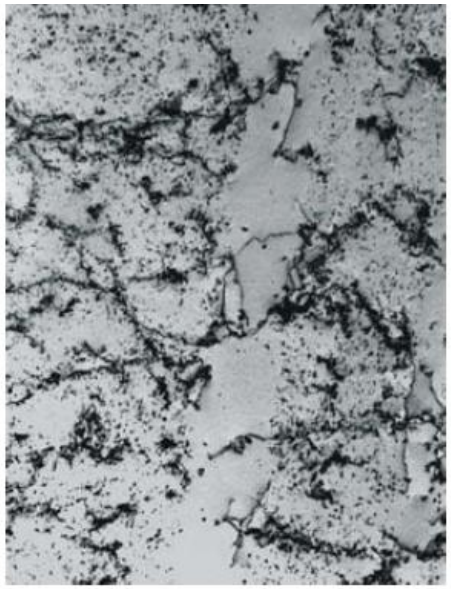

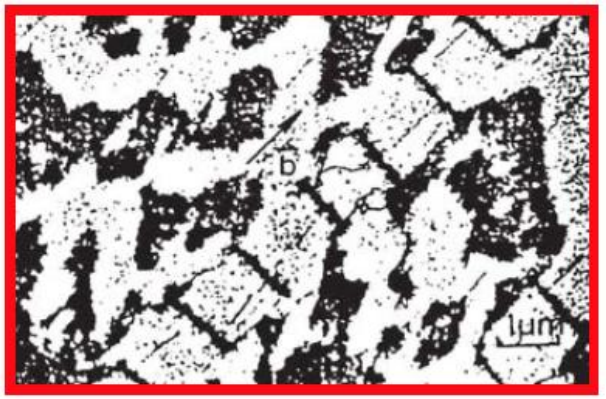
b
1μm

Bulk Phenomena

High Heat Flux/ Neutron flux/ Mechanical Loads result in:

Short timescale phenomena (e.g. 10^{-12} – 10^{-9} s):

- Atomic Displacements;
- Fast Transport;
- Lattice Defects (Vacancies and Interstitials).

Long timescale phenomena (e.g. 10^{-3} – 10^{6} s):

- Microstructure Evolution (Voids, Bubbles, Dislocations, Phases);
- Dimensional Instabilities (Swelling and Creep);
- Shear Bands (Localized plasticity);
- Helium Embrittlement.

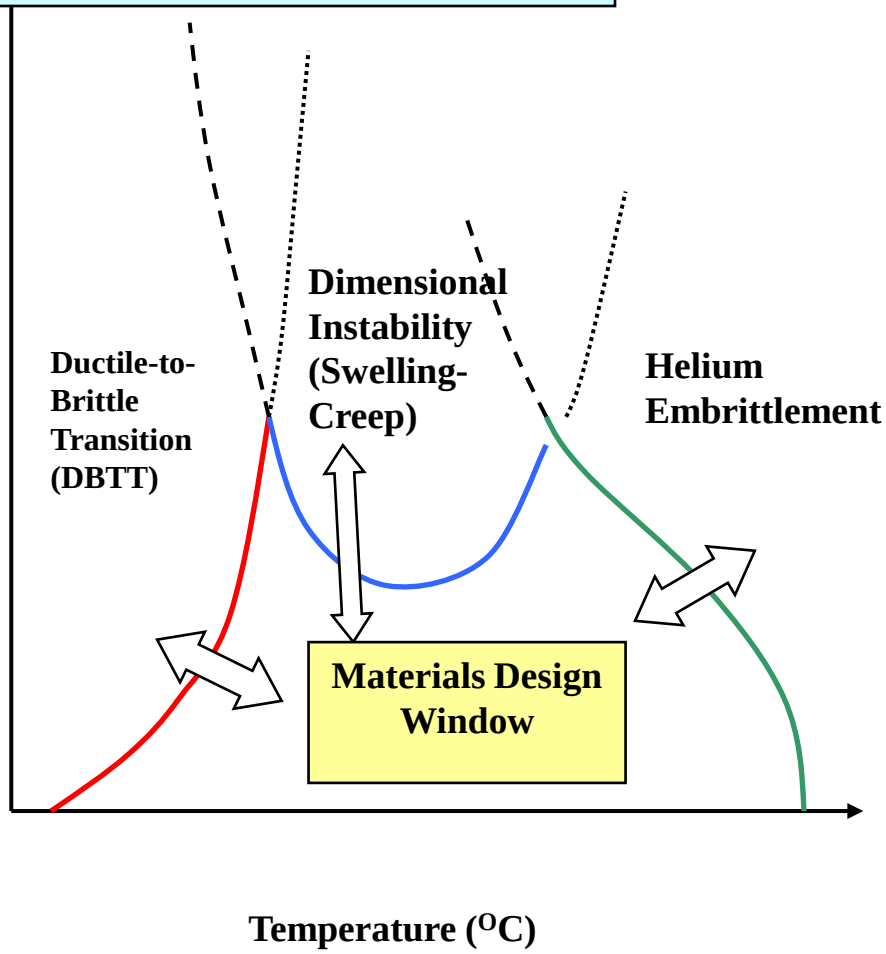

Atomistic Simulations*

First-principles

(<200 atoms,<10ps)

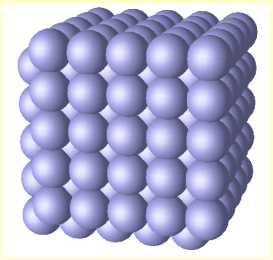

- Start from Schroedinger's Equation;
- Approximate: DFT;
- Accurate energetics of point defects and defect clusters

Molecular dynamics

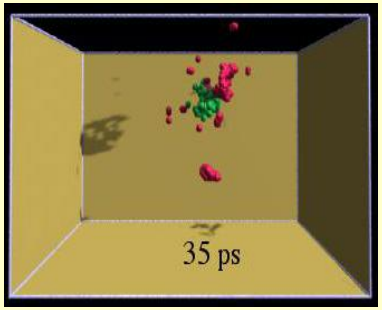

- Empirical Potentials;
- Initial defect distribution;
- Verlet or predictor-corrector;
- time-step ~ 1 fs;
- Short-range forces;
- Parallelization by spatial decomposition with MPI.
- (1-100 million atoms, < 100 ns)

KMC (<μm,<ms)

- Freeze atomic degrees of Freedom;
- Track defects only;
- Microstructure evolution of defects
- Spatial inhomogeneity.

* Srolovitz and Carr - Princeton

Atomic Displacements

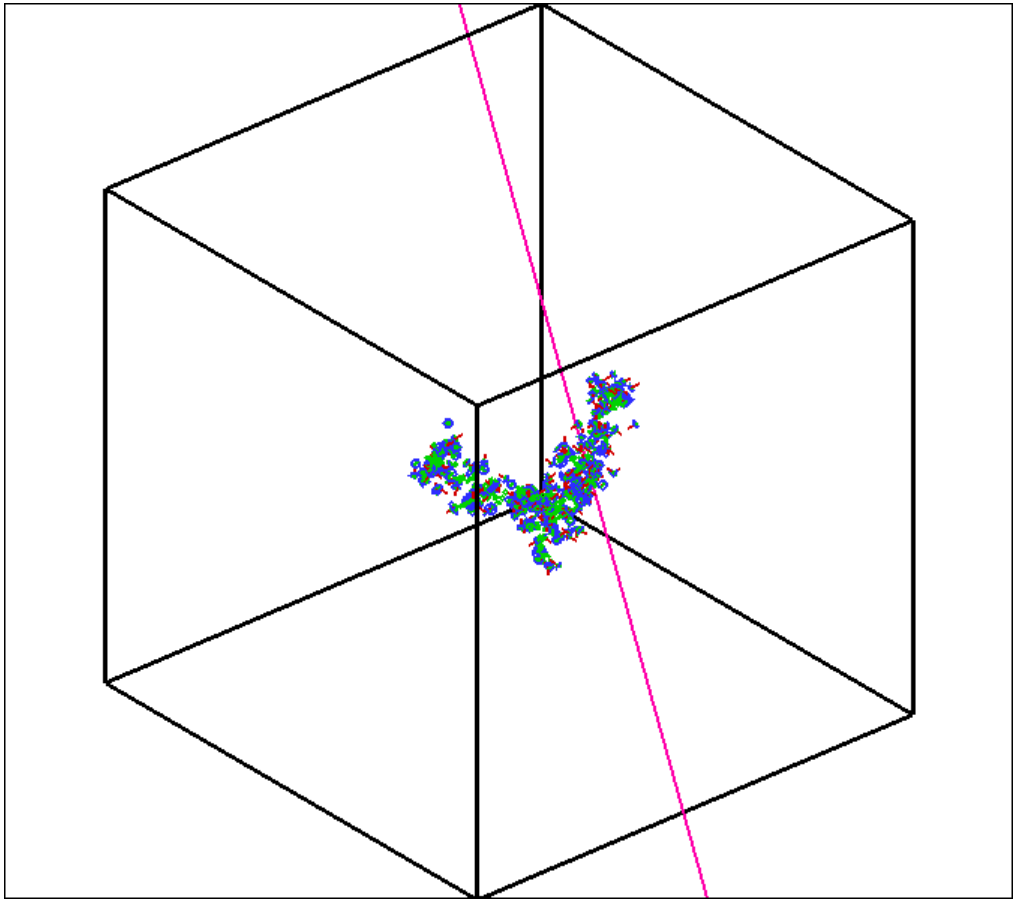

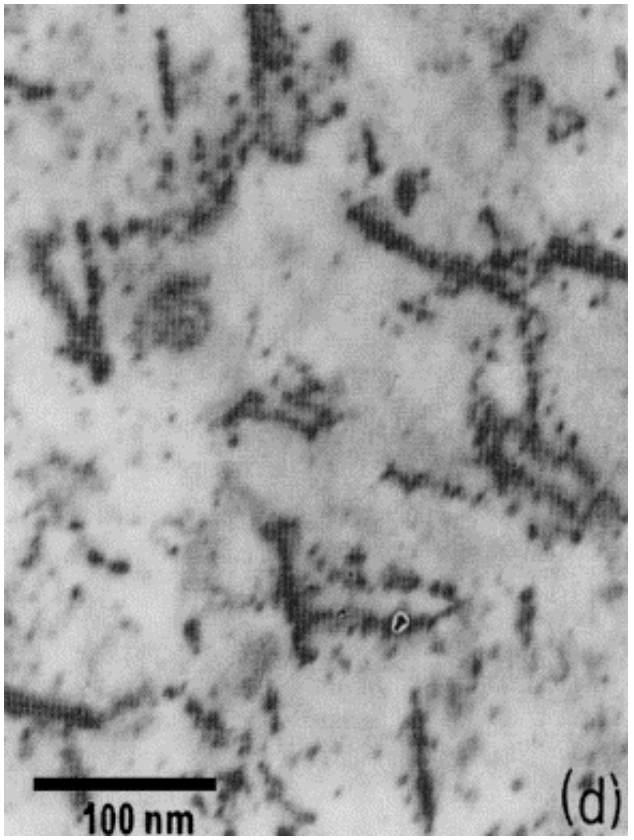

Radiation damage and defect cluster physics

- **Atomistic (molecular dynamics, molecular statics and kinetic Monte Carlo) simulations to investigate displacement cascade evolution (Fe-10%Cr), defect cluster structure & transport (Fe, Fe-He, Fe-Cr, V), cascade aging -**
  Collaborative effort with UCSB, ORNL, PNNL and Princeton (V)

20 keV cascade in Fe-10%Cr

QuickTime™ and a
Cinepak decompressor
are needed to see this picture.

<100> dislocation loop nucleation

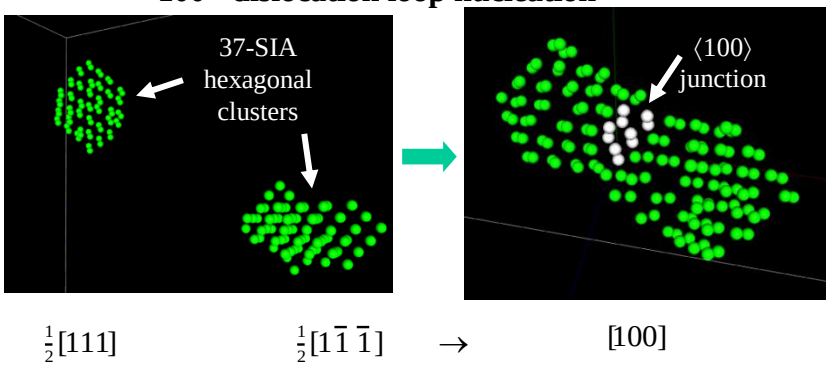

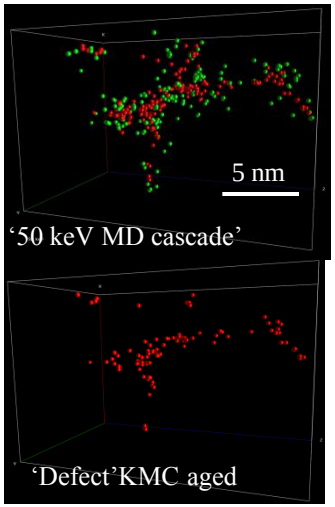

Cascade aging in Fe

Cascade energy (keV)	MD defects (~ 100 ps)	Surviving vacancies (~ 100 ns)
5	22.0	13.2 (60%)
10	33.9	20.2 (60%)
20	59.3	38.2 (64 %)
40	131	77.5 (59%)
50	168.3	90.9 (54%)
100	332.3	180.1 (54 %)

Fe displaced atom
Cr displaced atom
Vacancy

UCLA

Interatomic Potentials and MD Simulations

$$\mathcal{H}\Phi\{R_I, r_i\} = E_{tot}\Phi\{R_I, r_i\}$$

$$\mathcal{H} = \sum \frac{P_I^2}{2M_I} + \sum \frac{Z_I Z_J e^2}{R_{IJ}} + \sum \frac{p_i^2}{2me} + \sum \frac{e^2}{r_{ij}} - \sum \frac{Z_I e^2}{|R_I - r_i|}$$

- Born-Oppenheimer: Adiabatically eliminate nuclear degrees of freedom. Solve only for electrons.
- Kohn-Sham-Hohenberg: Density Functional Theory (DFT) reduces to the single electron quantum problem, with effective potentials.
- Exchange-Correlation potentials are approximated with the Local Density Approximation (LDA).
- Using DFT-LDA material properties have been calculated without input.

Quantum MD

Bond-order Potentials

Stoller, ORNL

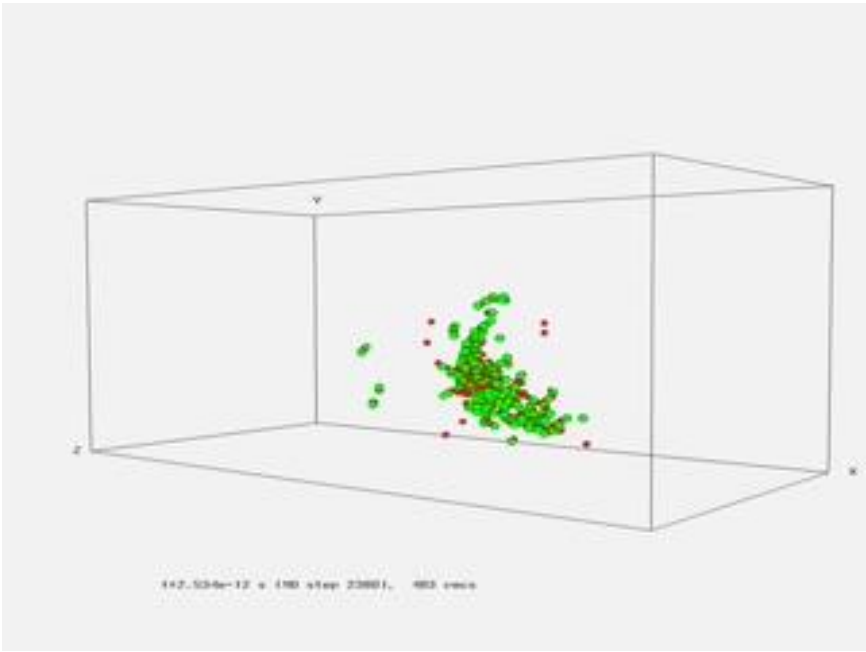

$$\frac{d^2 R_I}{dt^2} = F_I = -\frac{dV}{dR_I}, \qquad \mathcal{H} = \sum \frac{P_I^2}{2M_I} + V(R_I)$$

$$E = \sum_i \left\{ F_i(\bar{\rho}_i) + \sum_{j \neq i} \frac{1}{2}\Phi_{ij}(r_{ij}) \right\} \qquad F_i = A_i E_i^0 \bar{\rho}_i \ln \bar{\rho}_i$$

Classical MD with Empirical Potentials

Response of Fe-Cr Alloys to Irradiation

- **Fe-Cr ferritic/martensitic steels and dispersion strengthened variants are candidate structural materials for high(er) temperature fission and fusion applications**

Phase diagram

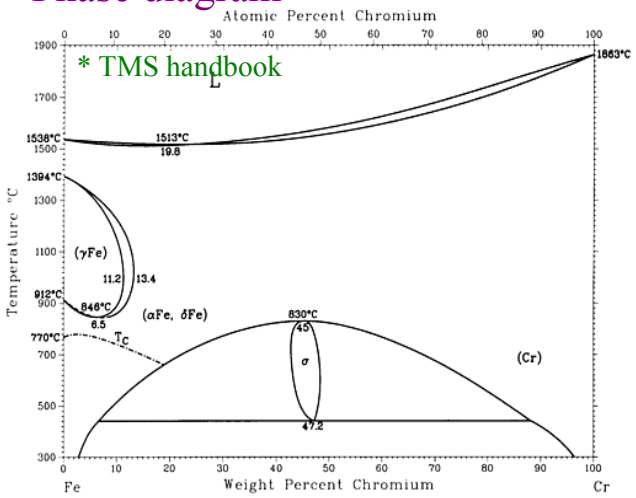

* TMS handbook

Resistivity recovery, SIA-Cr

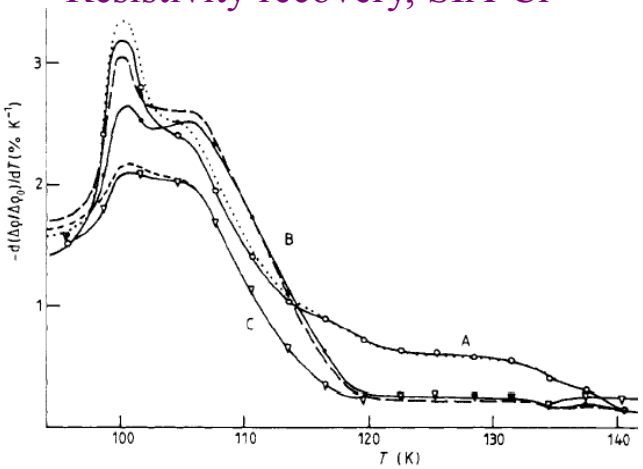

* F. Maury et al., *J. Phys F* **17** (1987)

Dislocation loops

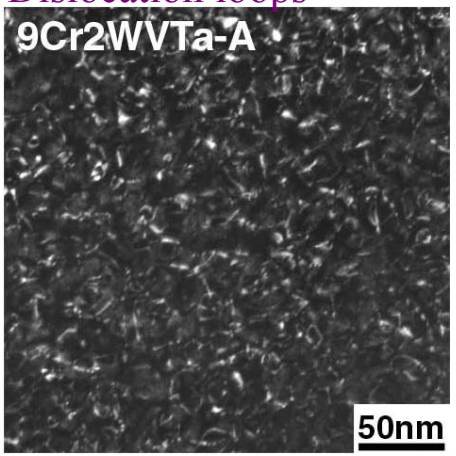

* N. Hashimoto et al., MRS **650** (2000)

Grain boundary segregation of Cr

F82H
Proton irradiated
250°C, 0.5 dpa:

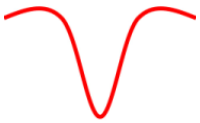

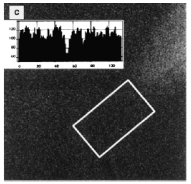

Fig. 3. Chemical mapping of the F82H material irradiated at 0.5 dpa at 523 K. (a) Zero loss image, (b) Fe map and (c) Cr map. The inserts show the image profile integrated in the respective boxes outlined in white. Horizontal axis is in pixels, vertical axis in counts.

* R. Schaeublin et al., *JNM* **258-263** (1998)

HCM12A
Ni+ irradiated
500°C, 5 dpa:

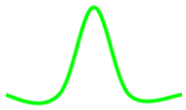

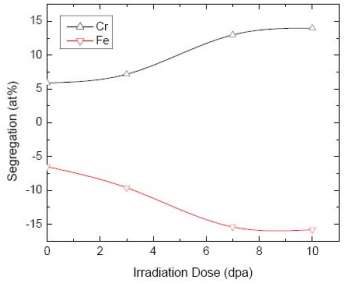

* T.R. Allen et al., 22nd ASTM

Understand Cr - point defect interactions, Cr segregation behavior and microstructural evolution

Semi-empirical potentials: Size effects

Finnis-Sinclair potentials: $E_{tot} = \frac{1}{2}\sum_{i \neq j}^{n} V_{ij}(R_{ij}) - \sum_{i}^{n}\left\{\sum_{j}^{n}\phi_{ij}(R_{ij})\right\}^{1/2}$

Fe: Ackland et al., Phil. Mag. (1997)

Cr: Finnis and Sinclair, Phil. Mag. (1984)

For Fe-Cr:
Konishi et al., Comp. Mater. Sci. (1999)

$$\phi_{FeCr} = \alpha\sqrt{\phi_{FeFe}\phi_{CrCr}}$$

$$V_{FeCr} = \frac{\beta}{2}\left(\frac{\phi_{FeCr}}{\phi_{FeFe}}V_{FeFe} + \frac{\phi_{FeCr}}{\phi_{CrCr}}V_{CrCr}\right)$$

α and β fit to experimental data

Substitutional Cr atom

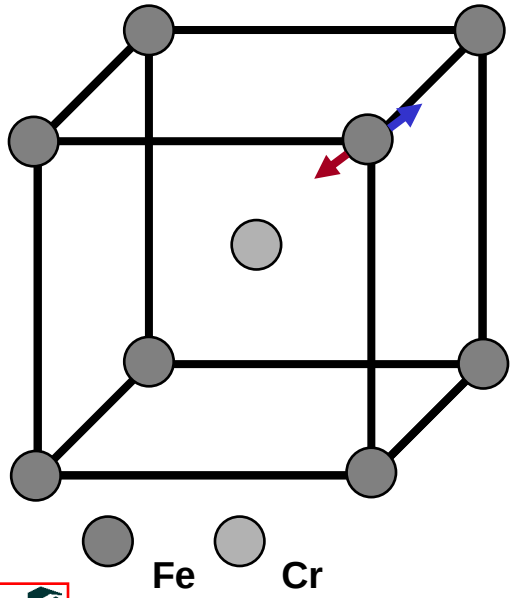

1st NN change (%)

FeCr I	**+0.53**
FeCr II	**-0.32**
Ab-initio (LCAO)	**-0.29**
Ab-initio (VASP)	**-0.08 - -0.5**

Cr concentration 1.8%

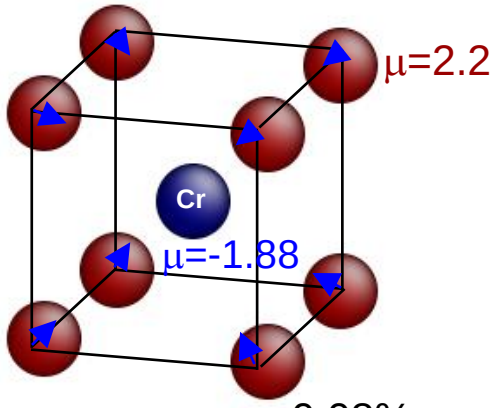

0.08% contraction

FeCr II potential in reasonable agreement with ab-initio predictions for size effects, but not Vac-Cr binding energy. FeCr I potential in better agreement for SIA-Cr interactions.

J.-H. Shim, H.-J. Lee and B.D. Wirth, *J. Nucl. Mater* **351** (2006) 56.

Point defect - Cr binding energy

Cr - Vacancy	E_b (eV)		
1NN	0.04	-0.002	0.044
2NN	-0.04	-0.01	-0.005
	Fe-CrI	Fe-CrII	VASP

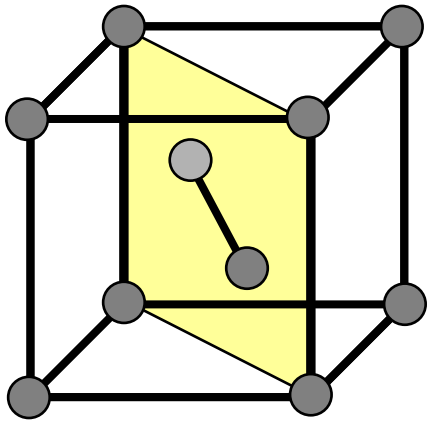

E_b (eV)

FeCr I -0.25

FeCr II +0.20

Ab-initio +0.37*

<111> mixed dumbbell

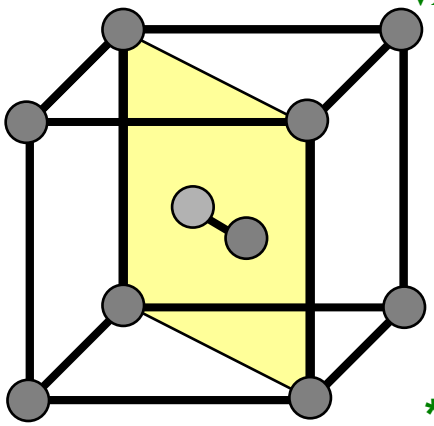

E_b (eV)

FeCr I -0.40

FeCr II +0.10

Ab-initio 0.08*

*P. Olsson, et al.

<110> mixed dumbbell

● Fe ● Cr

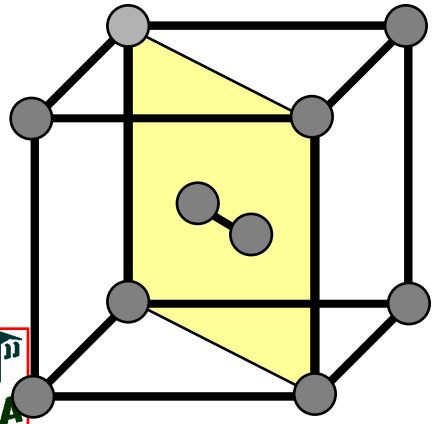

E_b (eV)

FeCr I -0.16

FeCr II +0.06

Ab-initio +0.05*

<110> db + parallel Cr

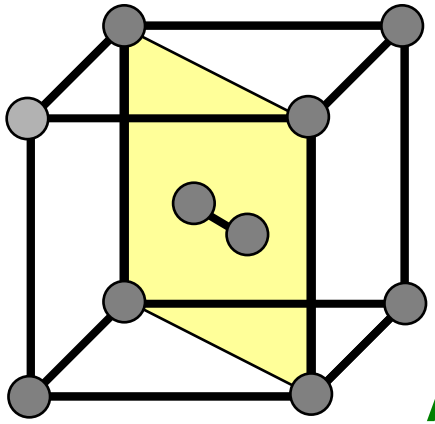

E_b (eV)

FeCr I +0.02

FeCr II -0.01

Ab-initio -0.08*

<110> db + perpendicular Cr

Screw dislocation-SFT interaction in FCC Cu

•Snapshots of SFT and screw dislocation interaction process at τ_{xy}=300MPa

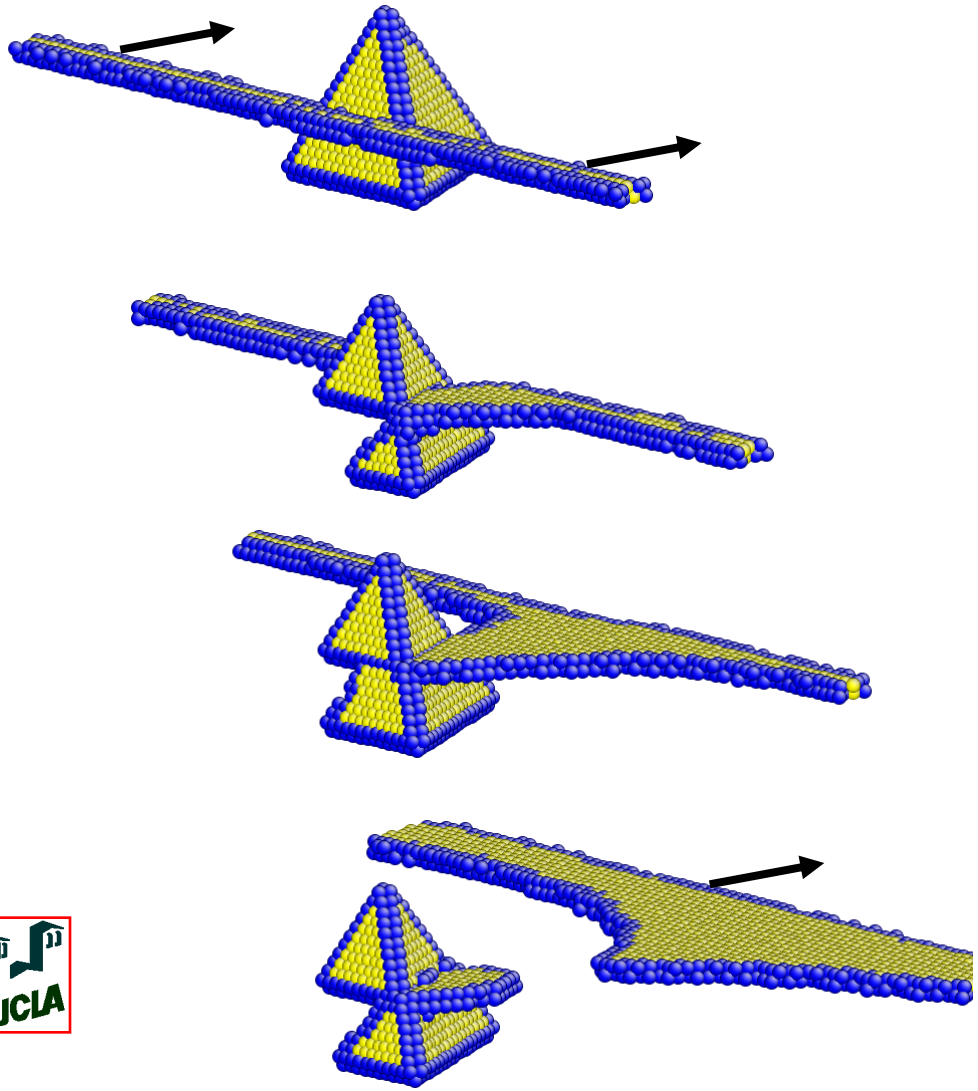

•Remaining structure immediately after the interaction

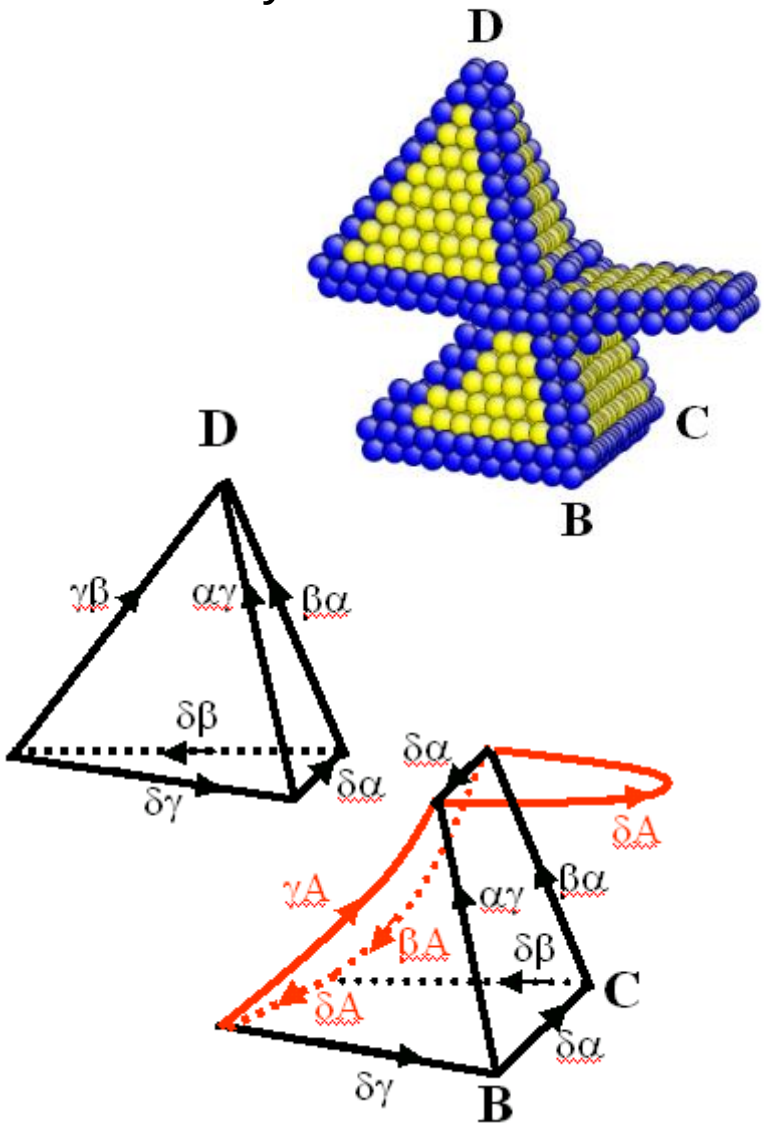

Comparison to in-situ TEM results

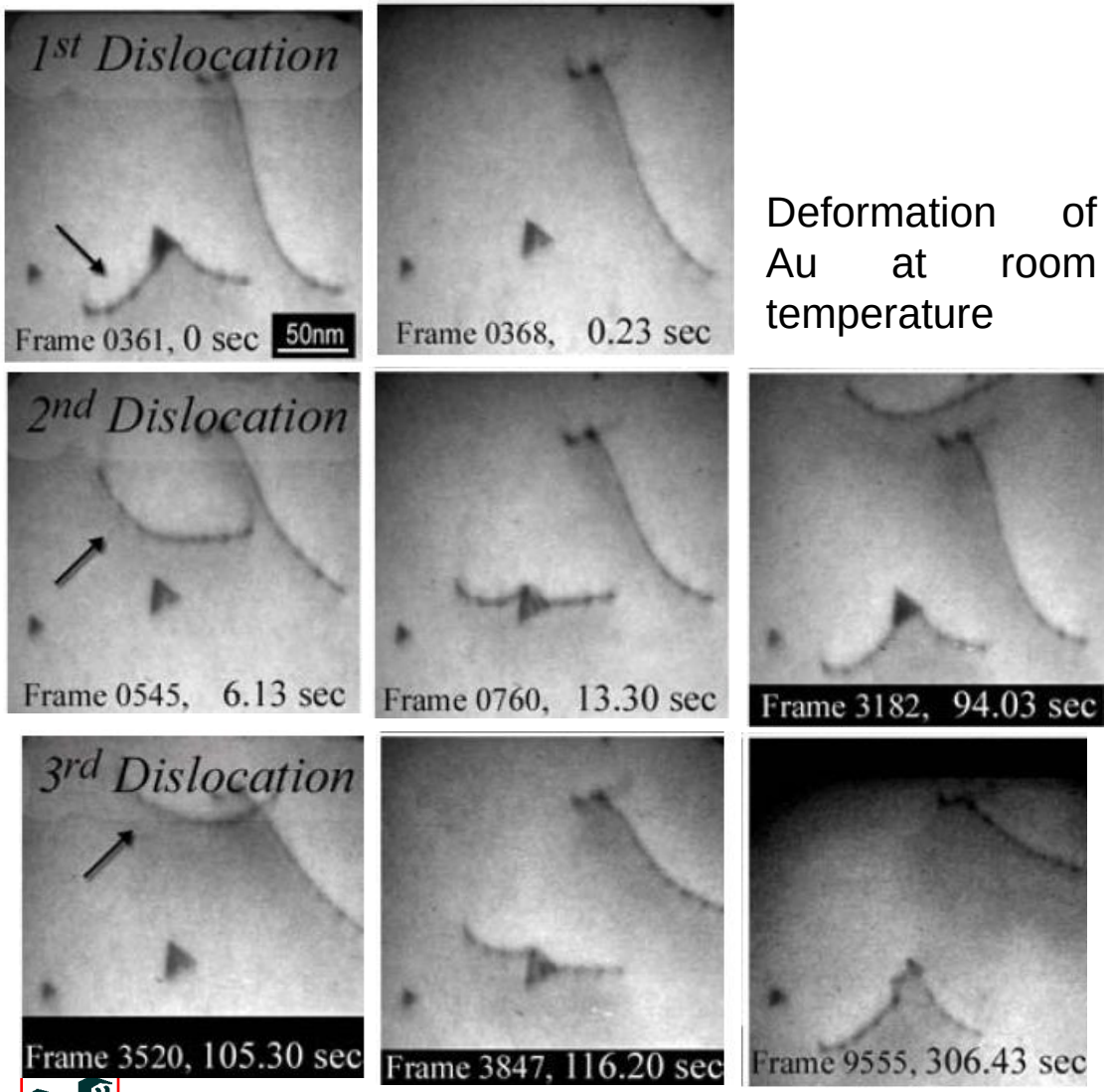

Deformation of Au at room temperature

Screw dislocation

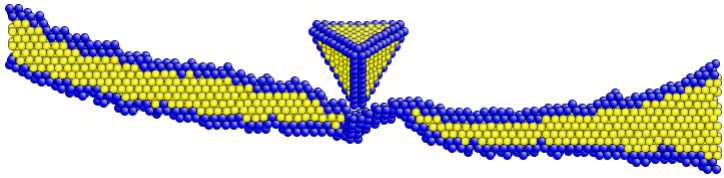

Edge dislocation

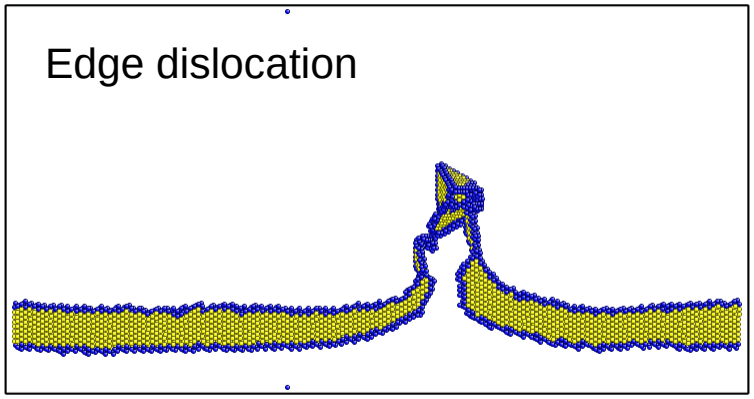

Mixed dislocation

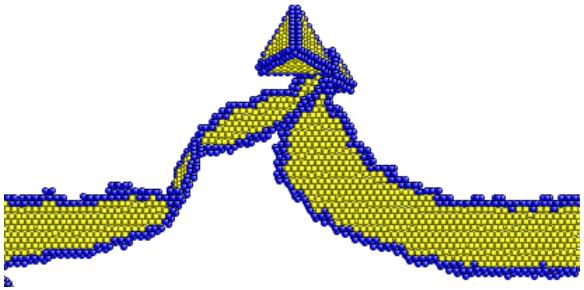

Ref: Y. Matsukawa et al., Journal of Nuclear Materials 329-333 (2004) 919.

Mesoscopic Simulations: Dislocation Dynamics

Covariant Vectors

$$(\mathbf{a}_1 = \mathbf{e},\ \mathbf{a}_2 = \mathbf{t},\ \mathbf{a}_3 = \mathbf{b}) \qquad \mathbf{e} = \frac{\mathbf{R}}{R} \qquad \mathbf{t} = \frac{\mathbf{T}}{T} \qquad \mathbf{T} = \frac{d\mathbf{l}}{dw}$$

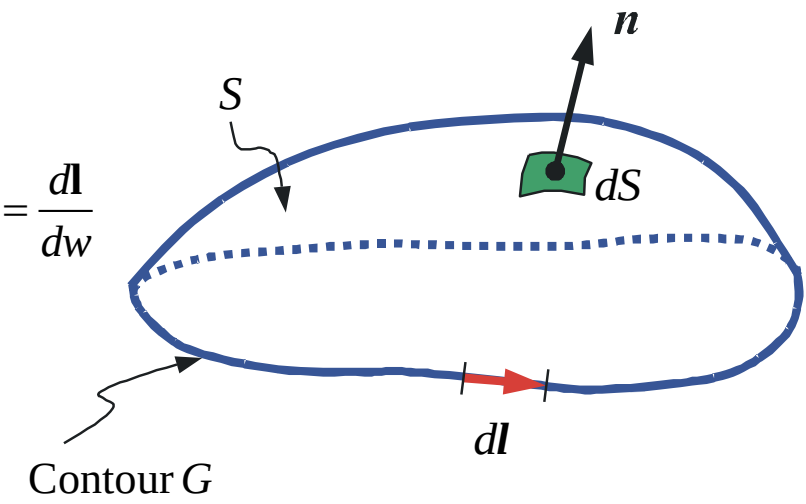

Contravariant Vectors

$$\mathbf{a}^1 = \frac{1}{2\pi V}(\mathbf{a}_2 \times \mathbf{a}_3)$$

$$\mathbf{a}^2 = \frac{1}{2\pi V}(\mathbf{a}_3 \times \mathbf{a}_1)$$

$$\mathbf{a}^3 = \frac{1}{2\pi V}(\mathbf{a}_1 \times \mathbf{a}_2)$$

$$V = (\mathbf{a}_1 \times \mathbf{a}_2) \cdot \mathbf{a}_3$$

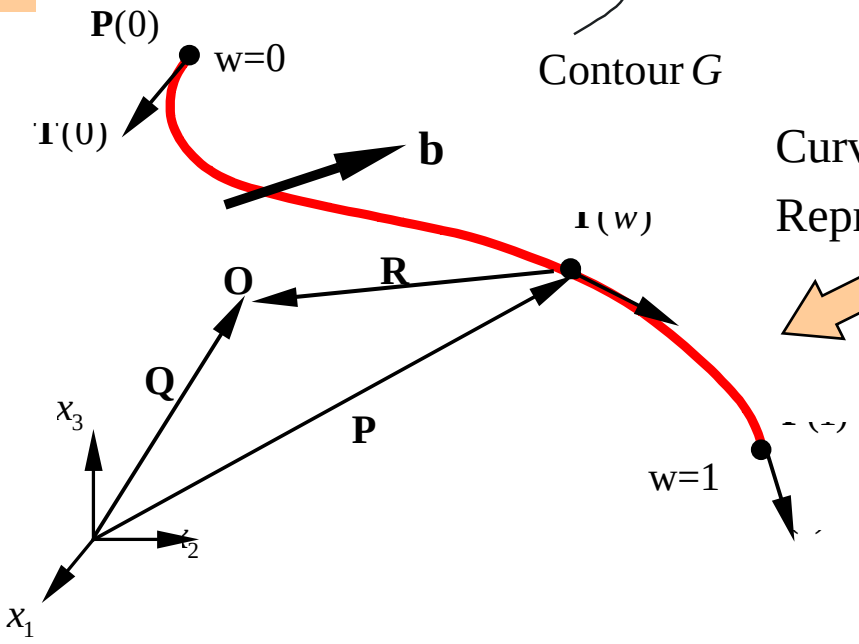

Curved dislocation segment
Represented by a spline

Differential Forms of DD are analogous to Electromagnetics, but of higher dimensionality

Biot-Savart

$$d\vec{B} = \frac{\mu_o}{4\pi}\frac{Id\vec{s}\times\hat{r}}{r^2}$$

Displacement

$$\frac{d\mathbf{u}}{dw} = \frac{T}{4R}\left\{\frac{(\mathbf{s}\times\mathbf{a}_1)\cdot\mathbf{a}_2}{\pi(1+\mathbf{s}\cdot\mathbf{a}_1)}\mathbf{a}_3 + \frac{V}{1-\nu}\left[(1-2\nu)\mathbf{a}^1\right] + \frac{1}{2\pi}\mathbf{a}_1\right\}$$

Stress

$$\frac{d\boldsymbol{\sigma}}{dw} = \frac{\mu VT}{2R^2}\left\{\frac{1}{1-\nu}\left(\mathbf{a}^1\otimes\mathbf{a}_1 + \mathbf{a}_1\otimes\mathbf{a}^1\right) + \left(\mathbf{a}^2\otimes\mathbf{a}_2 + \mathbf{a}_2\otimes\mathbf{a}^2\right) - \frac{1}{2\pi(1-\nu)}\left(\mathbf{a}_1\otimes\mathbf{a}_1 + \mathbf{I}\right)\right\}$$

Interaction Energy

$$\frac{dE_{\text{int}}}{dw_I dw_{II}} = -\frac{\mu T_I T_{II}}{4\pi R}\left[\begin{array}{l}\left(\mathbf{a}_2^I\cdot\mathbf{a}_3^I\right)\left(\mathbf{a}_2^{II}\cdot\mathbf{a}_3^{II}\right) - \frac{1}{1-\nu}\left(\mathbf{a}_2^I\cdot\mathbf{a}_2^I\right)\left(\mathbf{a}_3^I\cdot\mathbf{a}_3^I\right) \\ + \frac{2\nu}{1-\nu}\left(\mathbf{a}_2^{II}\cdot\mathbf{a}_3^I\right)\left(\mathbf{a}_2^I\cdot\mathbf{a}_3^{II}\right) - \frac{1}{1-\nu}\left(\mathbf{a}_2^I\cdot\mathbf{a}_2^{II}\right)\left(\mathbf{a}_3^I\cdot\mathbf{a}_1\right)\left(\mathbf{a}_3^{II}\cdot\mathbf{a}_1\right)\end{array}\right]$$

Weak Variational Form for DD Equations of Motion

Equations of Motion

$$\int_\Gamma \left(f_k^t - BV_k \right) \delta r_k ds = 0$$

$$\mathbf{v} = \frac{d\mathbf{r}}{dt}$$

$$\mathbf{f} = \mathbf{f}_{P-K} + \mathbf{f}_{self} + \mathbf{f}_{others}$$

Define:

$$\mathbf{r}^* = \frac{\mathbf{r}}{a}$$

$$\mathbf{f}^* = \frac{\mathbf{f}}{\mu a}$$

$$t^* = \frac{\mu t}{B}$$

Final Equation of Motion

$$\mathbf{K} \frac{d\mathbf{Q}}{dt^*} = \mathbf{F}$$

$$\mathbf{Q} = \left[\mathbf{P}_1, \mathbf{T}_1, \mathbf{P}_2, \mathbf{T}_2 \right]$$

Q=Nodal coordinate vector

F=Nodal Forces

K=Mobility Matrix

Mesoscopic Simulations of Plasticity

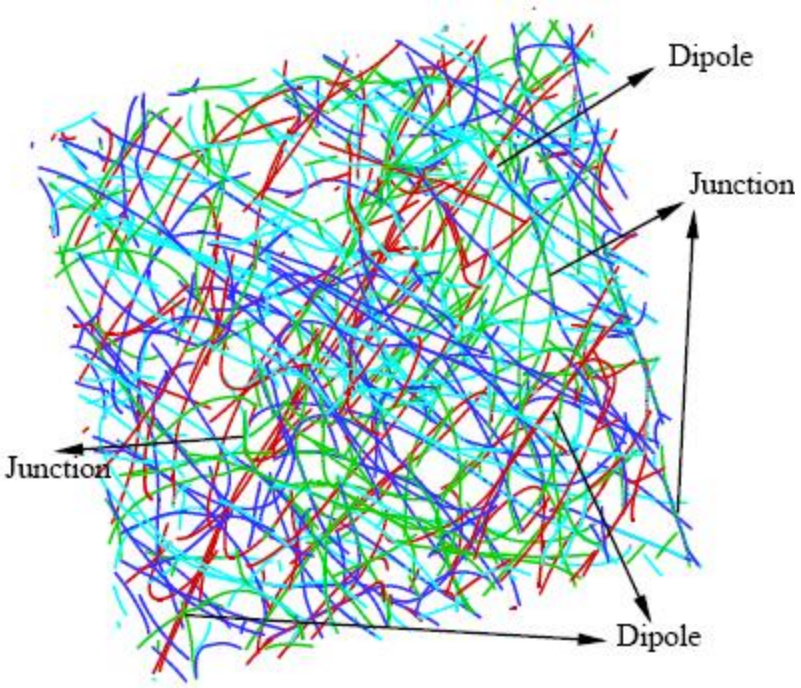

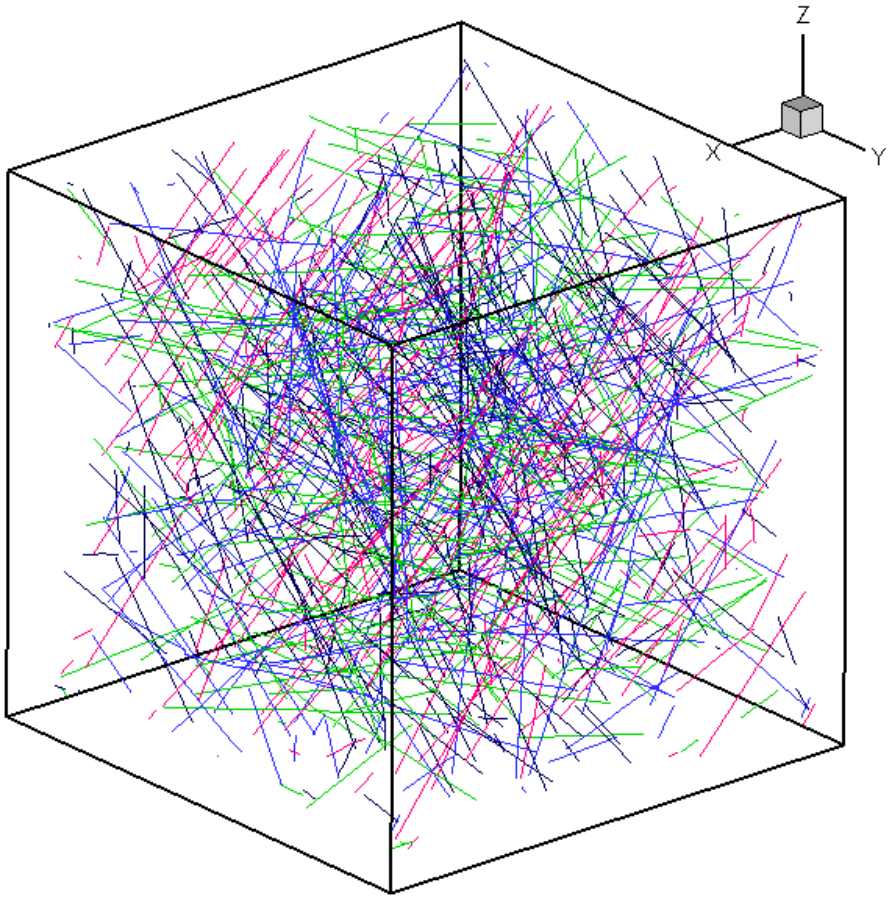

Microstructures (cont.)

Simulation volume size: 10μm x 10μm x 10μm

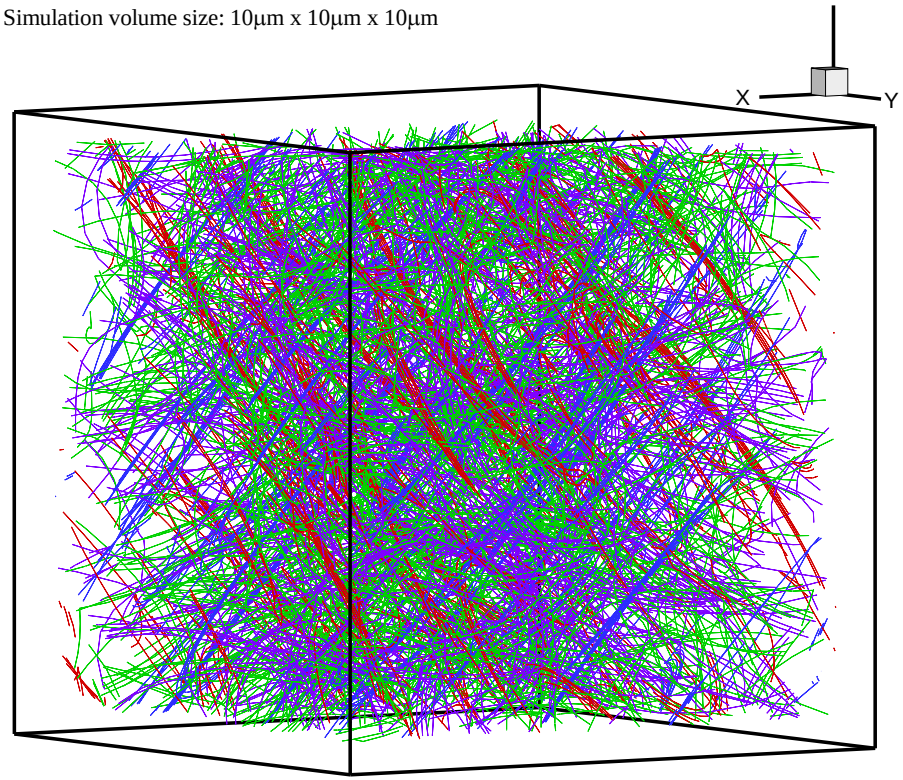

Simulation volume size: 10μm x 10μm x 10μm

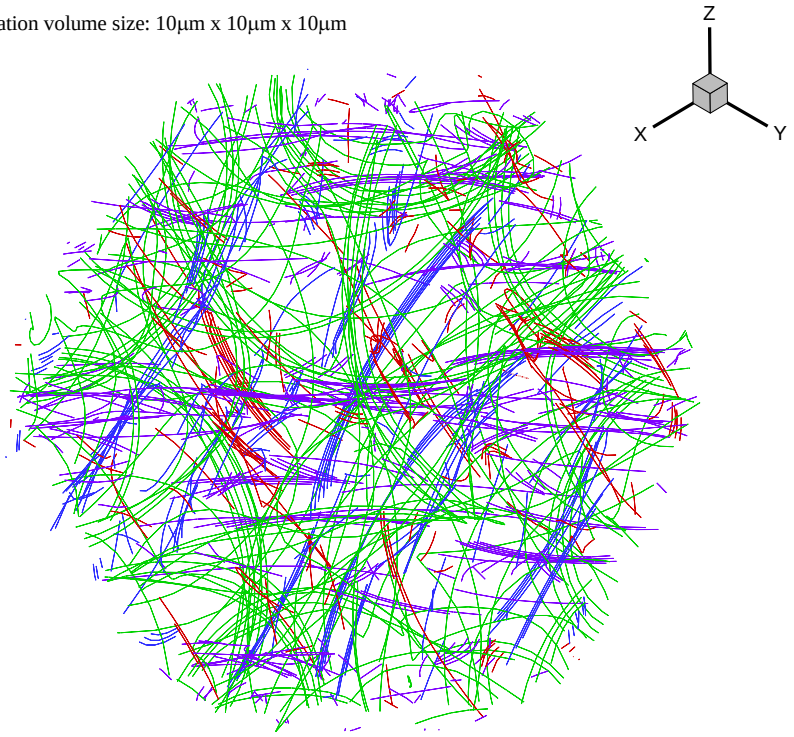

$$D = 7.5 \times 10^{8}\, cm/cm^{3}$$

Slice thickness: 2 micrometers

Radiation Increases Strength & Reduces Ductility (embrittlement)

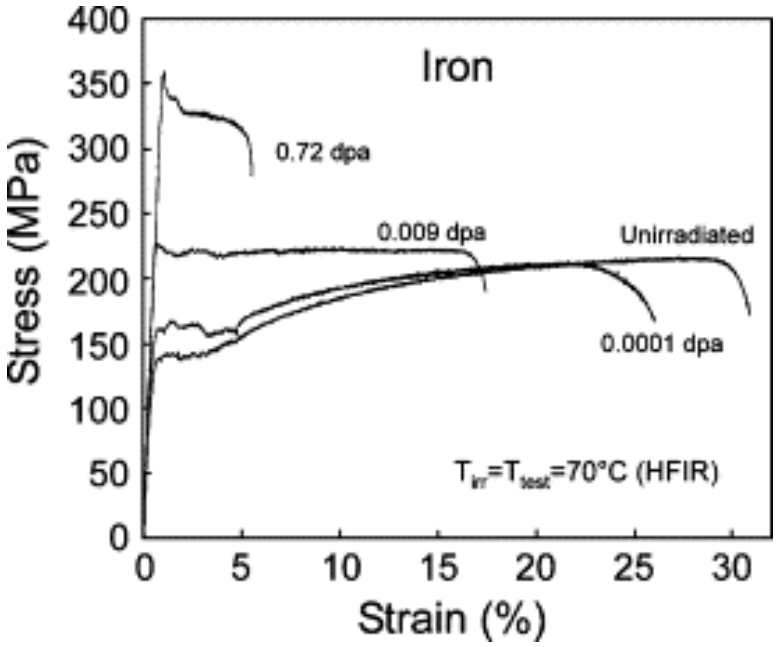

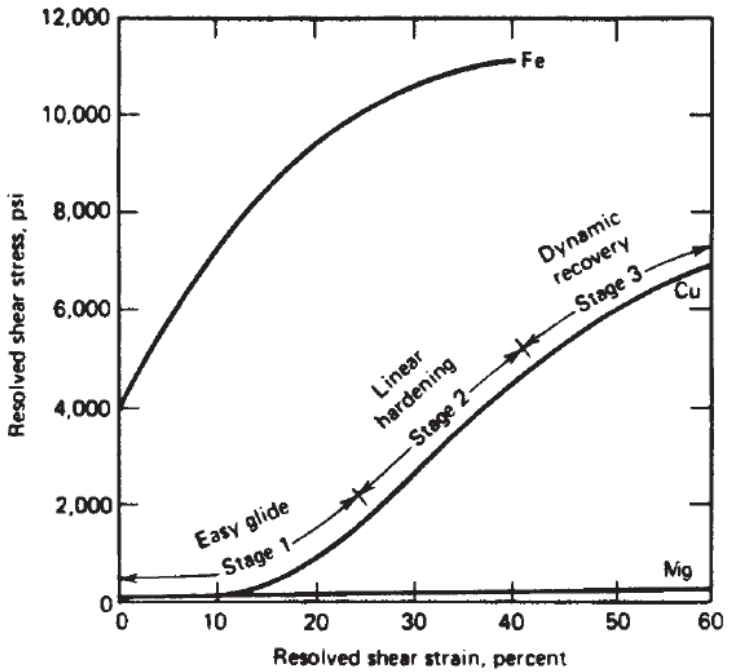

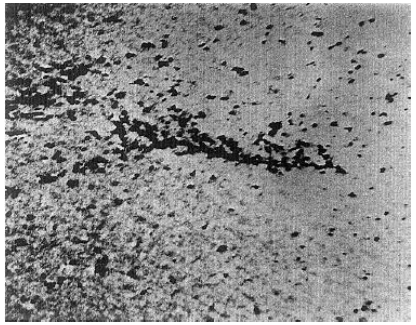

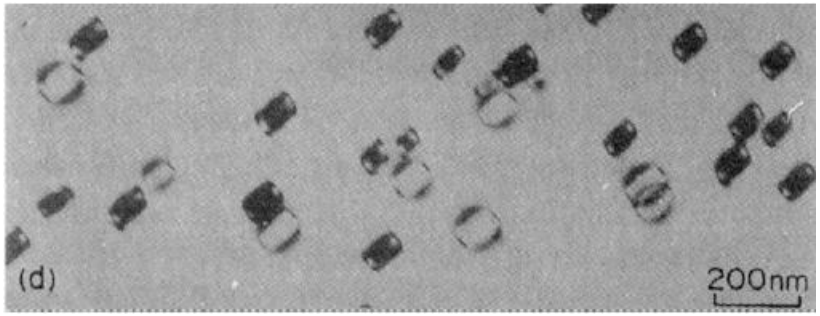

Continuum Modeling of Microstructure Instabilities and Self-Organization

Dose (isotropic)

Dose (anisotropic)

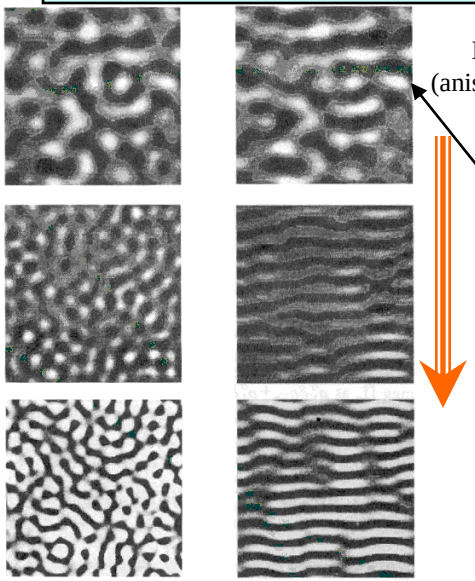

Simulations & experiments on self-organization of irradiated Cu microstructure.

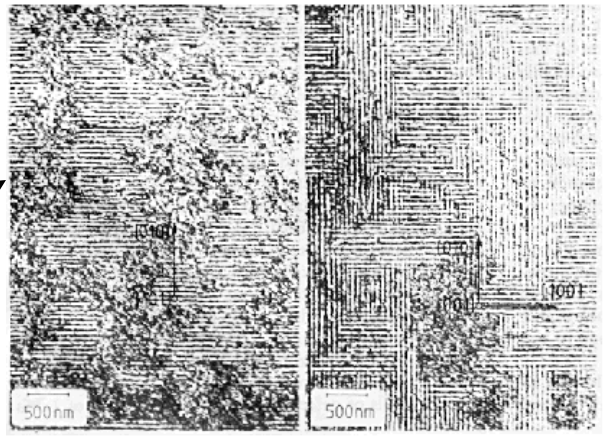

Ginzburg-Landau Dynamics Give Amplitude Equation for Patterns; bc= critical bifurcation Parameter

$$\tau_0 \partial_t A_i = \left[\frac{b - b_c}{b_c} - 4(\mathbf{q}_i \cdot \nabla)^2 \right] A_i + v \Sigma_{j,k} \overline{A}_j \overline{A}_k - 3u A_i (|A_i|^2 + 2\Sigma_{j \neq i} |A_j|^2) ,$$

Continuum Rate Equations for concentrations

$$\partial_t c_i = K(1-\epsilon_i) - \alpha c_i c_v + D_i \nabla^2 c_i - D_i c_i (Z_{iN}\rho_N + Z_{iV}\rho_V + Z_{iI}\rho_I) ,$$

$$\partial_t c_v = K(1-\epsilon_v) - \alpha c_i c_v + D_v \nabla^2 c_v - D_v [Z_{vN}(c_v - \overline{c}_{vN})\rho_N + Z_{vV}(c_v - \overline{c}_{vV})\rho_V + Z_{vI}(c_v - \overline{c}_{vI})\rho_I] ,$$

$$\partial_t \rho_I = \left[\frac{2\pi N}{|\mathbf{b}|} \right] [\epsilon_i K + D_i Z_{iI} c_i - D_v Z_{vI}(c_v - \overline{c}_{vI})] ,$$

$$\partial_t \rho_V = \frac{1}{|\mathbf{b}| r_V^0} \{\epsilon_v K - \rho_V [D_i Z_{iV} c_i - D_v Z_{vV}(c_v - \overline{c}_{vV})]\}$$

UCLA

Surface Phenomena

High Heat Flux/ Particle Flux result in:

Short timescale phenomena (e.g. 10^{-12} – 10^{-9} s):

- Sputtering;
- Implantation of helium and tritium;
- Re-deposition and tritium co-deposition;
- Near-surface damage (collision cascades).

Long timescale phenomena (e.g. 10^{-3} – 10^{6} s):

- Atomic transport (e.g diffusion, trapping, adsorption, recombination and desorption);
- Surface roughening and re-structuring;
- Microstructure and phase evolution (e.g. voids, bubbles, dislocations, grains & new phases).

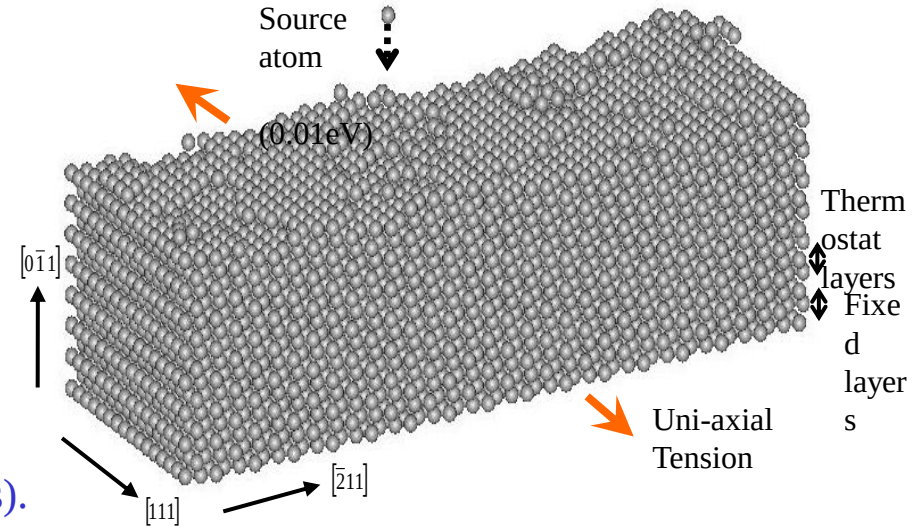

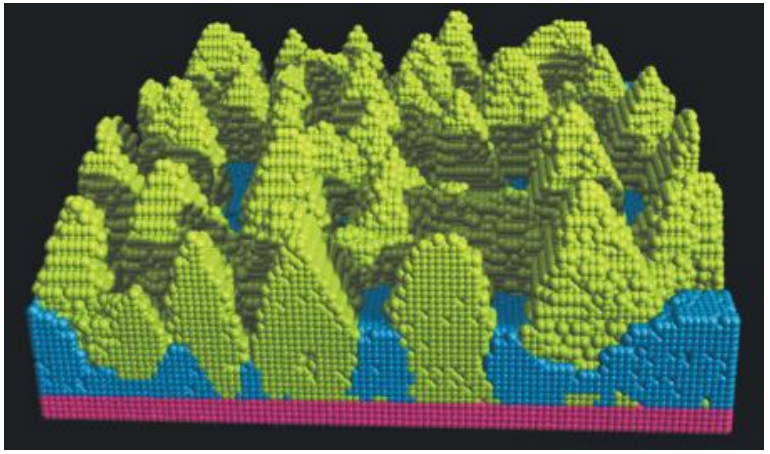

Surface Re-structuring after re-deposition.

H. Huang, RPI

Low Energy He-Bombardment

- ITER divertor plates are exposed to low temperature He, **$T_{He} < 100$ eV**
- ITER Helium fluxes are expected to be high: **~ 10^{20} - 10^{23} He/m^2-s**
- Tungsten displacement threshold energy: **E_d ~ 90 eV**;
- Tungsten surface energy barrier for helium implantation: **E_{SB} ~ 6 eV**
- Divertor Tungsten surface temperature: **600 < T < 1500°C**
- Although **$T_{He} < E_d$** , low energy He-bombardment experiments with Tungsten have shown significant surface morphology changes:
  - **High density of surface penetrating pores**
  - **High density sub-surface bubbles**
  - **Roughening**
  - **Formation of “cones” and “valleys”**

UCLA

Bubble Formation Process:

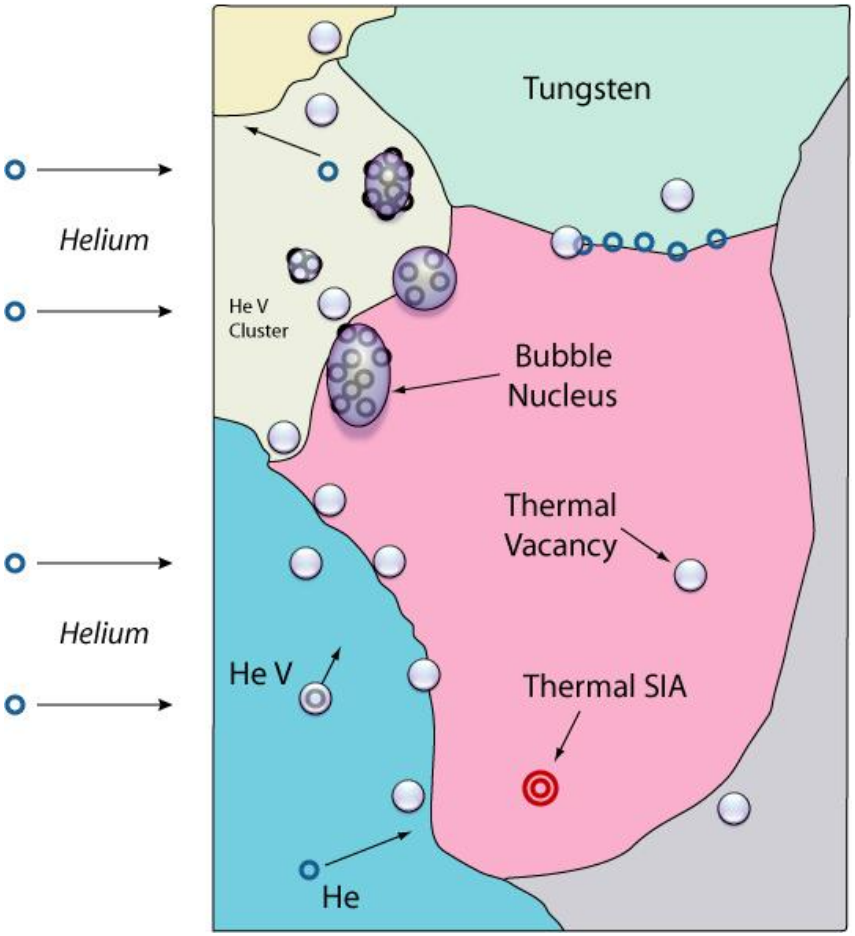

Bubble Growth Steps:

- Pre-existing "Thermal Vacancies" (C_v^e)
- Interstitial He arrives
- He is trapped in Vacancy
- Bubble Nucleus forms (<nm)
- Bubbles **pressurized** by He
- Vacancies form READILY on bubble surface
- Bubble grows by SIA emission

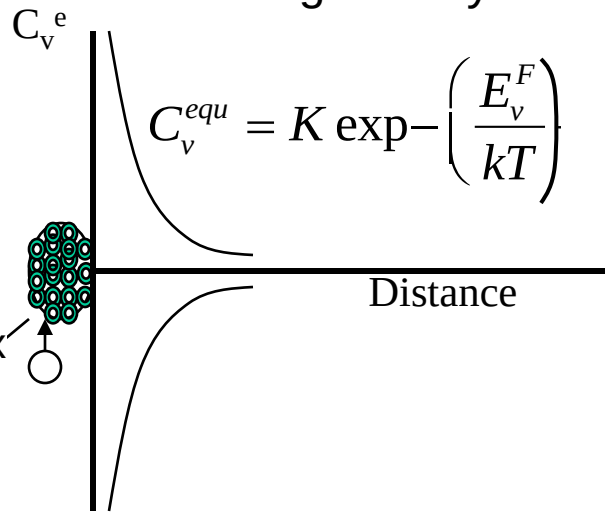

SIA is expelled from surface leaving behind a vacancy

Low Energy He Implantation in Tungsten:

Nishijima(2004)

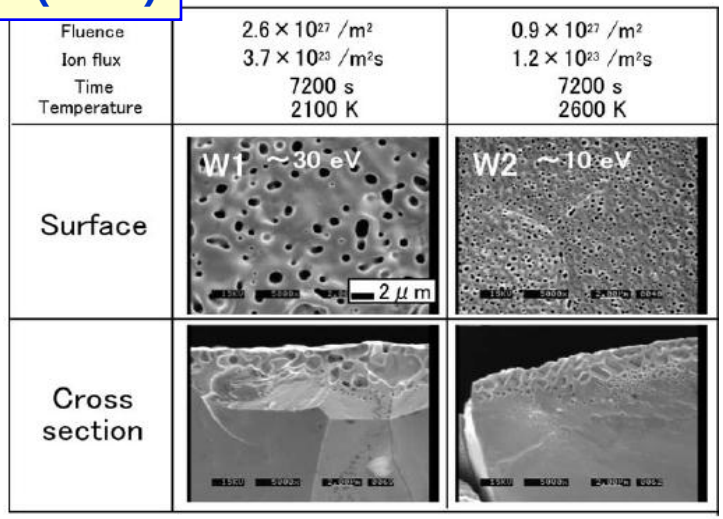

Tokitani (2005)

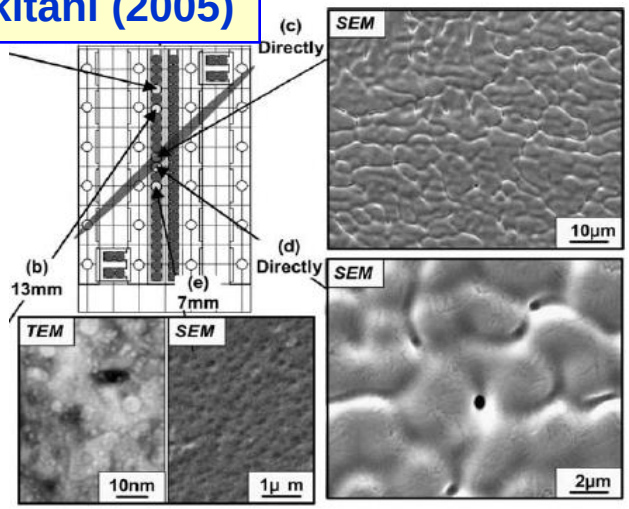

Tokunaga (2003)

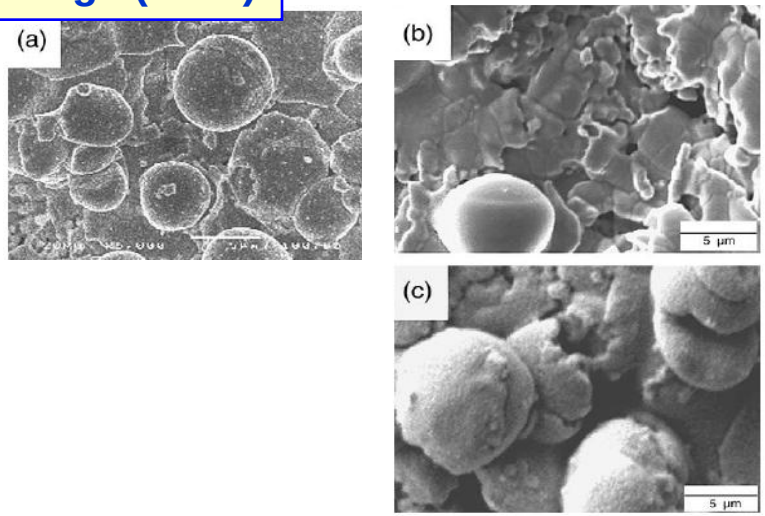

Iwakiri (2003)

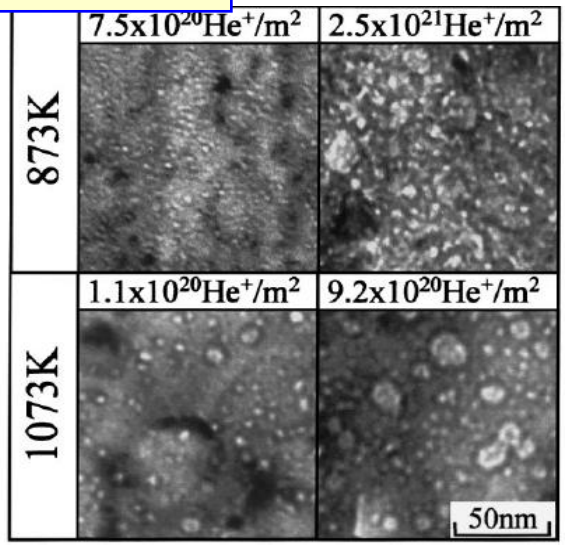

IEC Results (Cipiti & Kulcinski, 2004) :

Steady State:

40 KeV He

5×10^{18} $^4He/cm^2$

Temperature ⇑

Pore Size ⇑

Pore Density ⇓

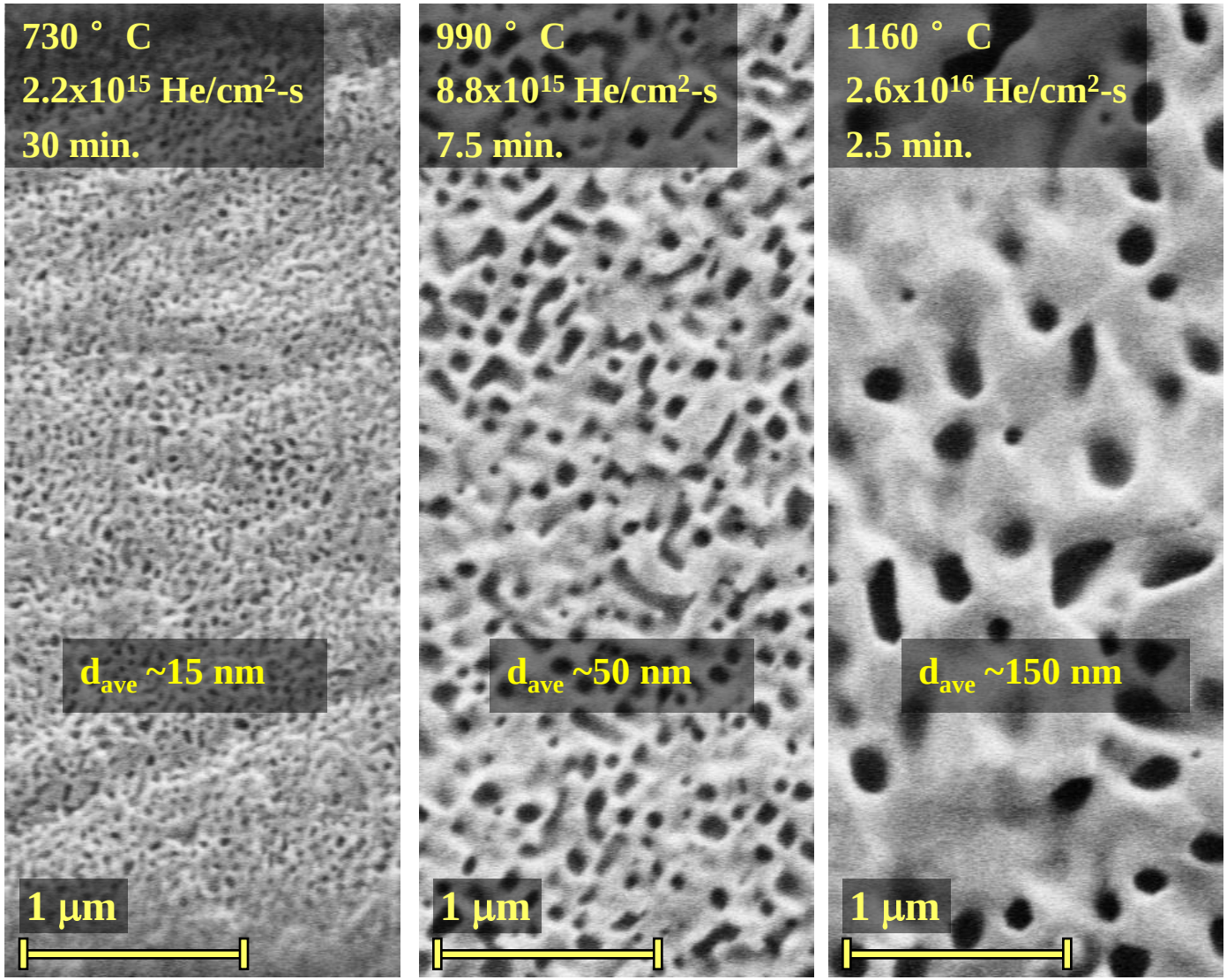

McHEROS Code Simulates IEC Surface Pores

	Temperature (°C)	Implantation Rate (He/cm²-s)	L_x (μm)	L_y (μm)	L_z (μm)
Model-1	730	2.2×10^{15}	0.2	1.0	1.0
Model-2	990	8.8×10^{15}	0.2	2.5	2.5
Model-3	1160	2.6×10^{16}	0.2	5.0	5.0

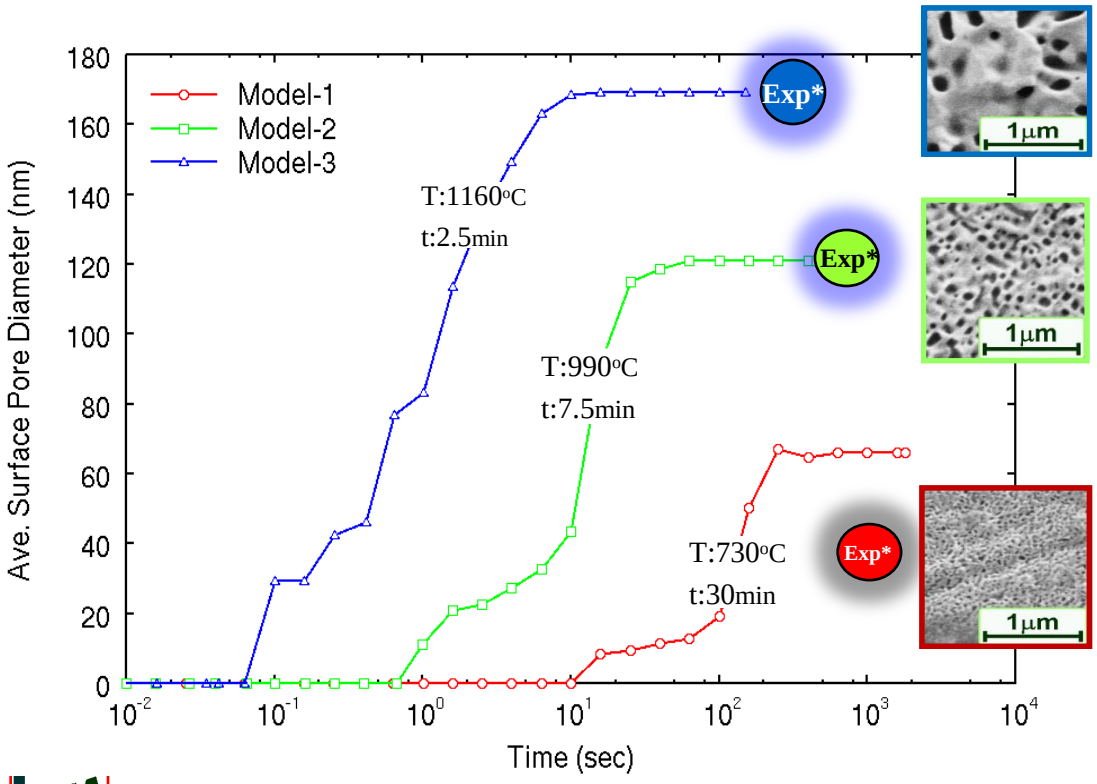

*Exp: IEC (UW-Madison)

2.2×10^{15} He/cm²-s; 730 °C; t:30min (IEC)

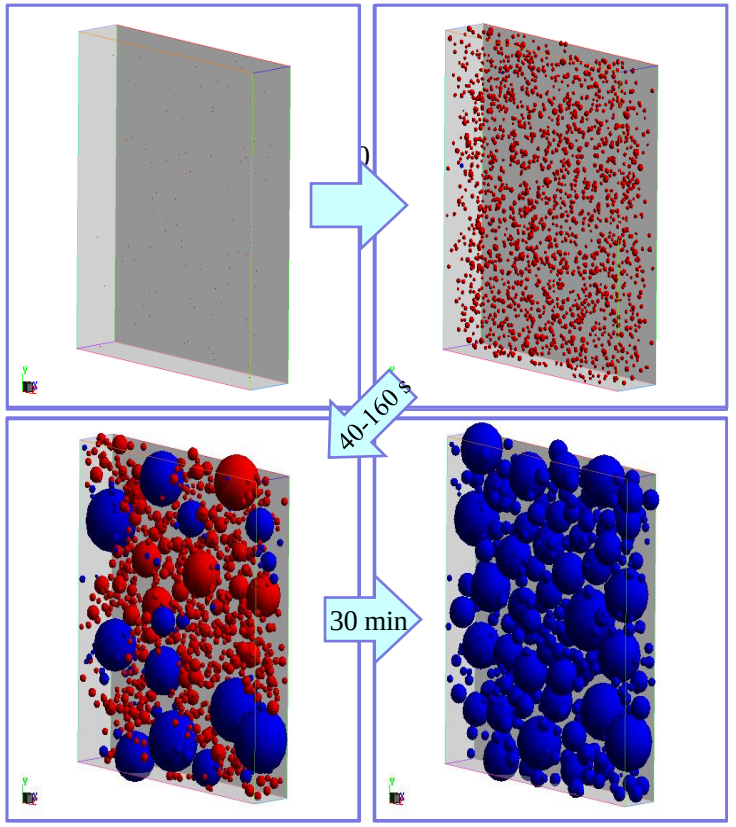

McHEROS Results:

- **Good Agreement between McHEROS Simulation and Experiment**
- **McHEROS provides an *EXPLANATION* for the oversized Surface Pores**

SiC vs. W: Ion profiles & Surface heating

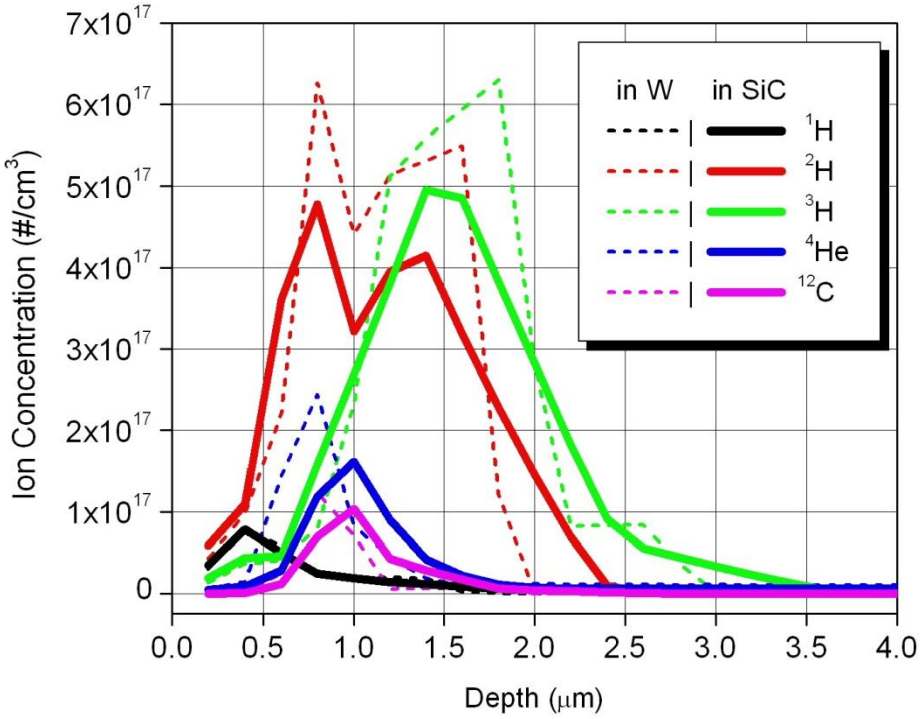

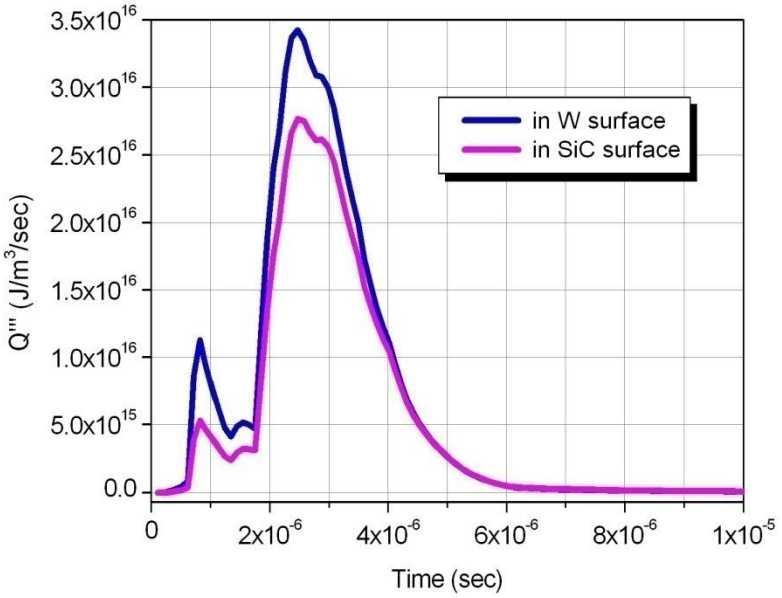

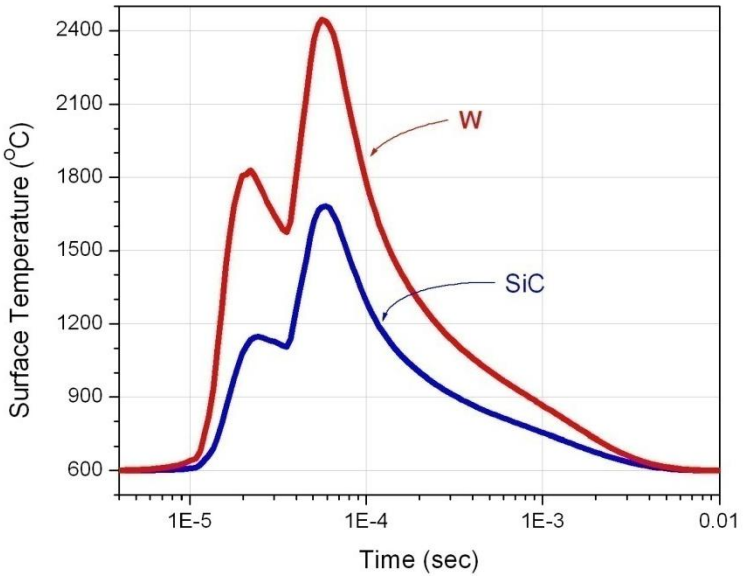

Single shot on W: stress & strain on surface

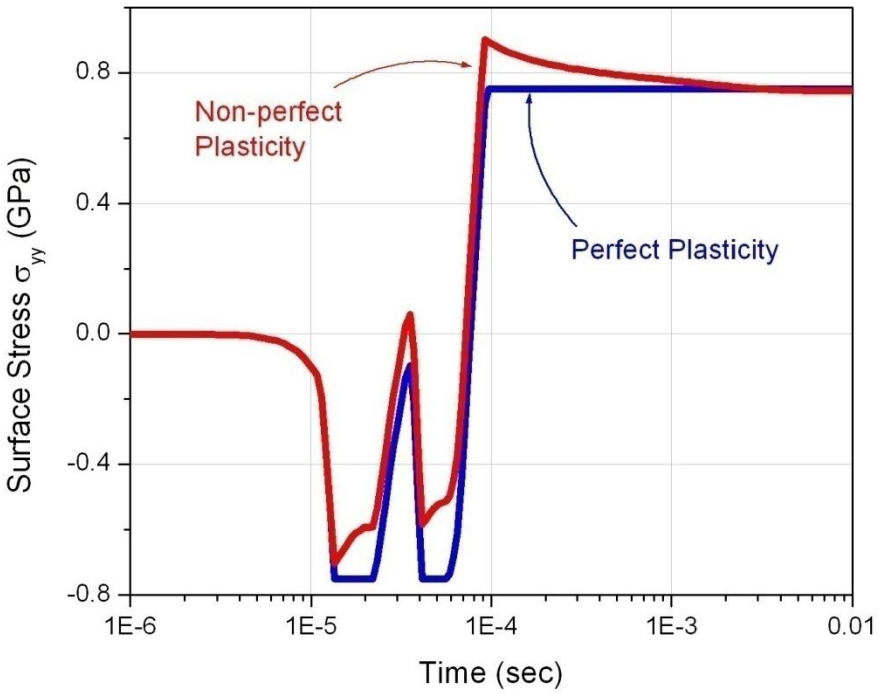

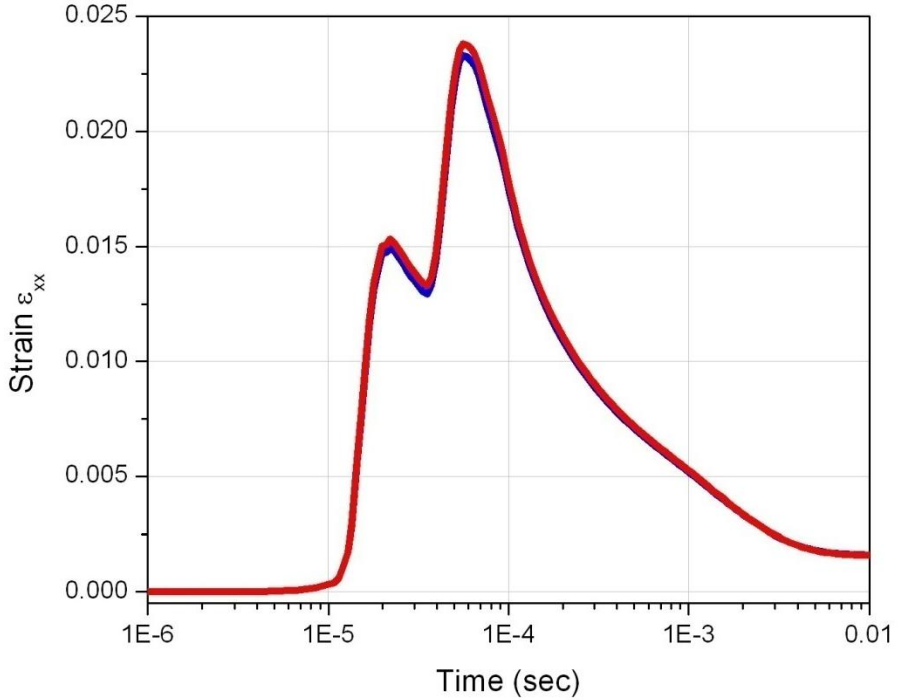

Roughening model produces surface profile similar to experimental results.

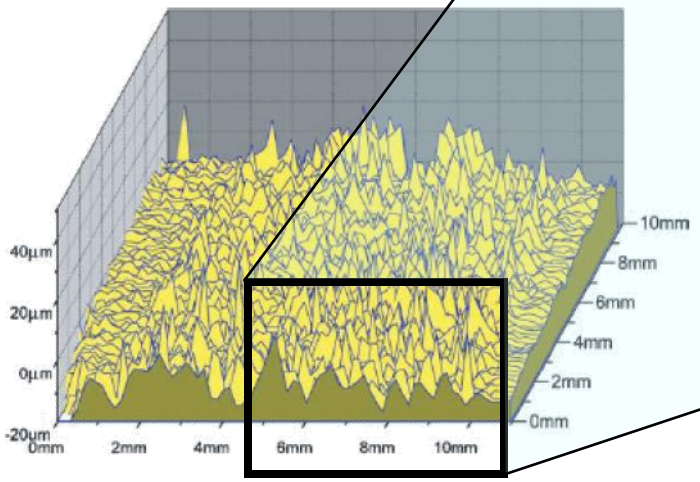

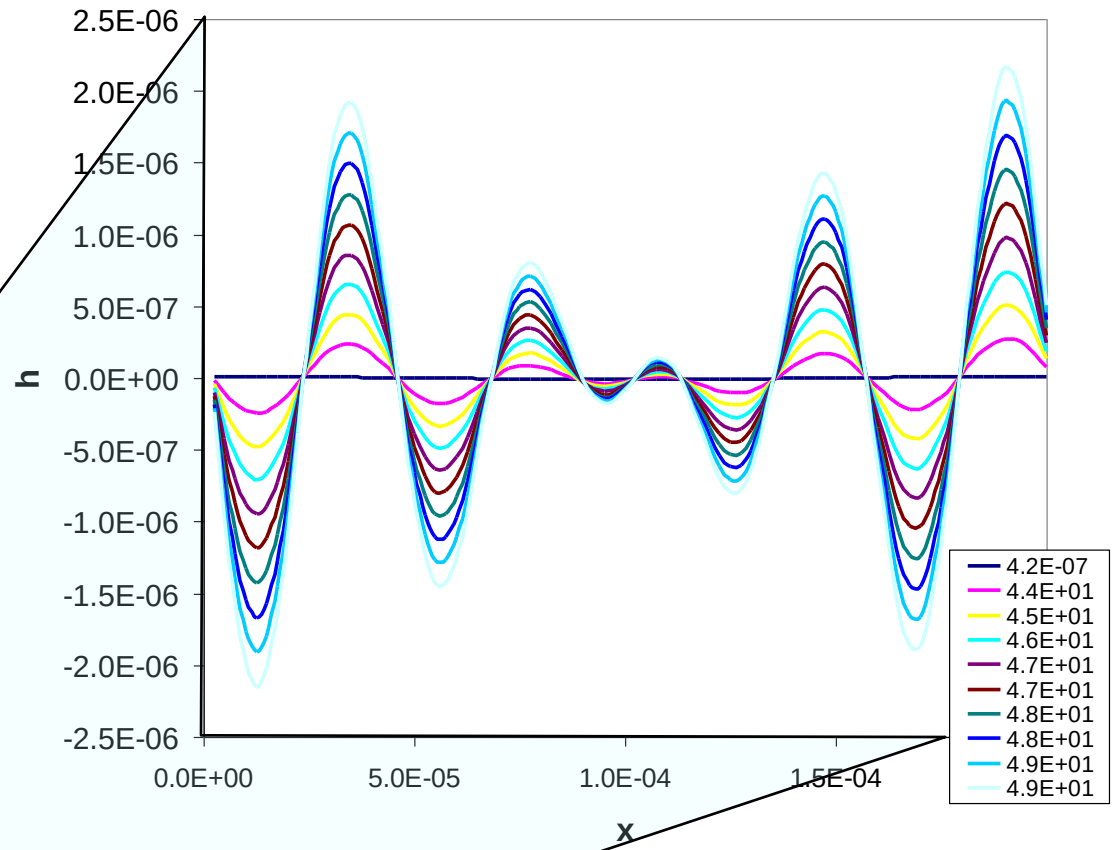

Critical depth reached after 49 seconds.

T.J. Renk JNM 2005.

Surface Crack Nucleation including Plasticity

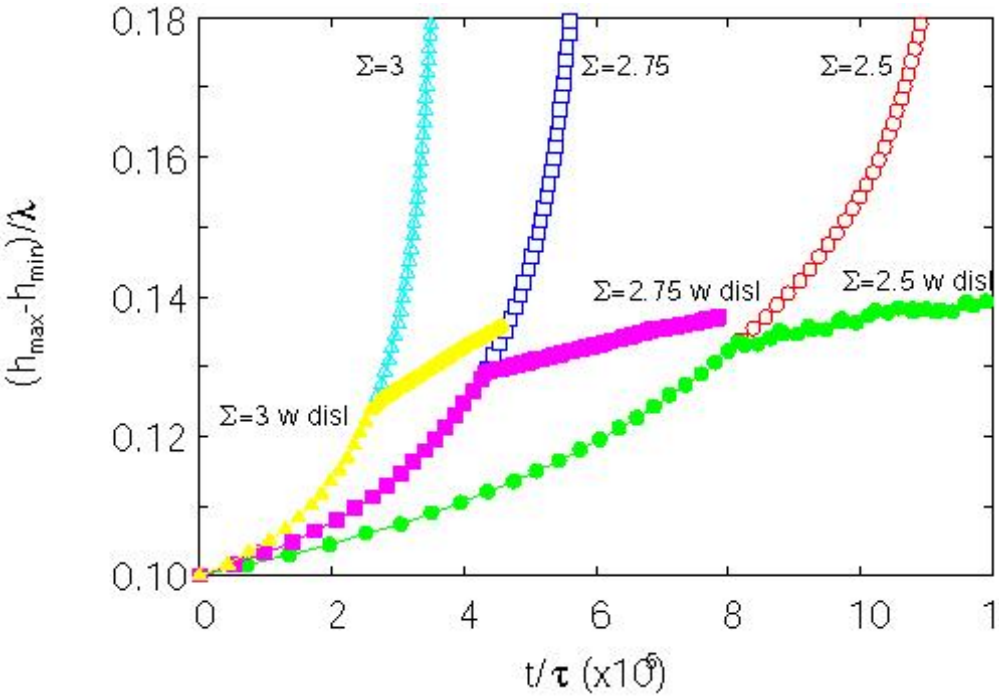

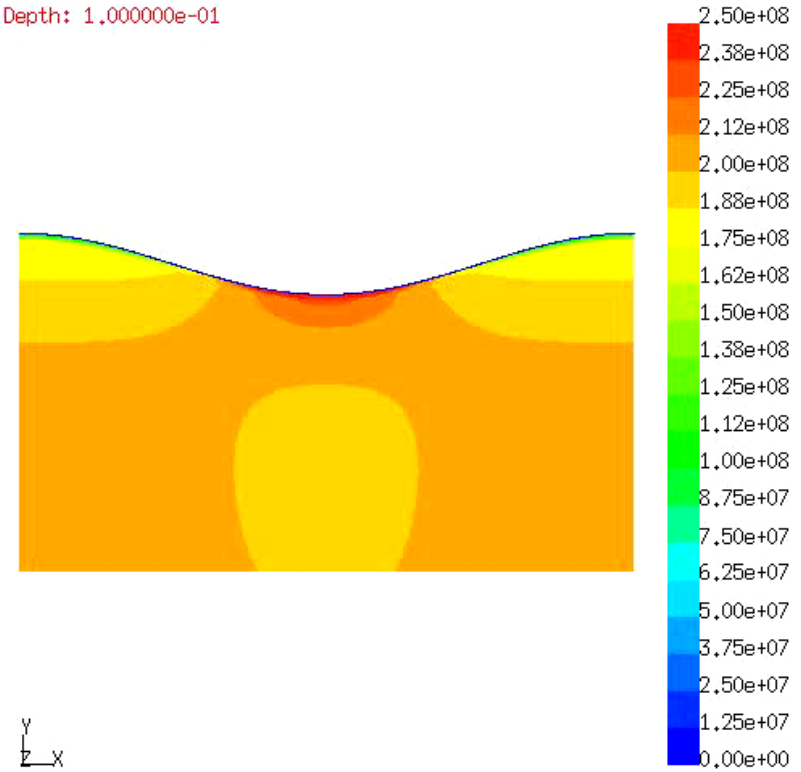

Curvature as a function of time.

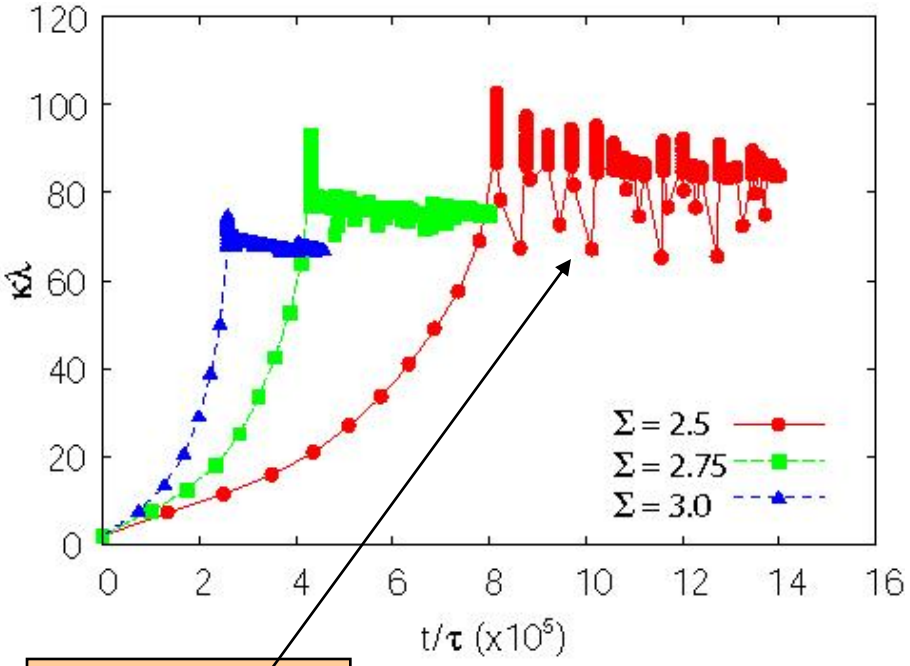

Blunting effect shown by drop in curvature.

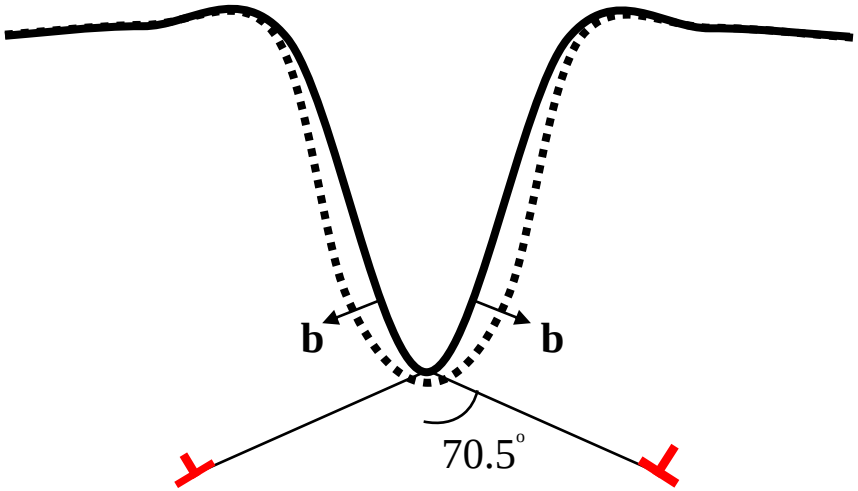

Super-dislocation containing 100 dislocation and 100 x Burgers Vector.